



*Università degli Studi della Basilicata*

Dottorato di Ricerca in “Sciences”  
*Curriculum “Chemical Sciences”*

***“Design, synthesis and biological evaluation  
of molecules for the treatment of SARS-CoV-2  
infection”***

*Settore Scientifico Disciplinare “CHIM-08”*

Coordinatrice del Dottorato  
Prof. Patrizia Falabella

Relatore  
Prof. Carmela Saturnino

Correlatore  
Prof. Magnus Monné

Dottoranda  
Dr. Federica Giuzio

Ciclo XXXVI

“Sapere che sappiamo quel che sappiamo, e sapere che non sappiamo quel che non sappiamo, questa è la vera conoscenza.”

NICCOLÒ COPERNICO

# CONTENTS

<b>ACKNOWLEDGMENTS</b>	<b>4</b>
<b>ABSTRACT</b>	<b>5</b>
<b>CHAPTER 1 - SARS-CoV-2 Infection and the Global Therapeutic Scenario</b>	<b>11</b>
1.1 The COVID-19 Pandemic	11
1.2 Drugs Used in Sars-CoV-2 Infection	13
1.3 Convalescent Plasma and Monoclonal Antibodies	15
1.4 Vaccines	16
1.5 Viral Variants	17
1.6 Spike Protein	19
1.7 Recent Studies for New Drugs	21
1.8 Potential Targets of Interest	23
<b>CHAPTER 2 - Aim of the Research</b>	<b>27</b>
<b>CHAPTER 3 - Potential PDE4B Inhibitors against SARS-Cov-2 Infection</b>	<b>30</b>
3.1 Introduction	30
3.2 Rationale for Molecular Docking Studies	34
3.3 Drug Likeness Predictions – Physicochemical - Pharmacokinetic/ADME Properties	42
3.4 Design of Human Transmembrane Protease Serine-2 (TMPS2) Inhibitors Guanidine Derivatives Against Sars-CoV2 Infection	48
<b>CHAPTER 4 – Results and Discussion</b>	<b>51</b>
4.1 Chemistry	54
4.2. In Vitro Studies	55
4.2.1. <i>Studies on Human PDE4B</i>	56
4.2.2. <i>Angiotensin II Converting Enzyme (ACE2) Inhibition Studies</i>	57
<b>CHAPTER 5 – Materials and Methods</b>	<b>60</b>
5.1 Chemistry	60
5.2. Human PDE4B Elisa Assay	60
5.3. Angiotensin II Converting Enzyme (ACE2) Inhibition Screening Studies	61
<b>CHAPTER 6 – CONCLUSIONS</b>	<b>62</b>
<b>REFERENCES</b>	<b>63</b>

## *Acknowledgments*

*My thanks go to Prof. Carmela Saturnino for the great support given in these three years and beyond, for her ability to convey the desire to discover, to understand and to reason. I thank Prof Magnus Monnè for teaching me to use docking programs that I would never have been able to imagine by observing molecules from the inside. I thank all those who have been close to me on this very tiring and painful journey for me, every single teacher of this University without any difference. From each one I received many notions and ideas for work. For me, the Covid years were not only years of PhD and study but also of field work, in the midst of the pandemic, with the fear of contracting an infection that we knew nothing about back in 2020. I feared the worst when I saw patients dying without the possibility of understanding how to save them and my experience in the field allowed me to become even more passionate about the study of this virus. I'm sure our work will be useful in the future...not too distant. Thanks to all those who supported me and a special thanks to Prof Abdallah Raweh with whom I conducted first in the United Arab Emirates in field hospital and then in Lugano one of the most important experiences of my life which will forever mark my path, as a woman, as a Medical Doctor, as a Researcher!*

## *Abstract*

SARS-CoV-2, responsible for the Coronavirus Disease-19 (COVID-19) infection, is an RNA virus belonging to the Coronavirus (CoV) family (1,2). Under the electron microscope, it appears like a crown (hence the name corona-virus): this characteristic is given by the presence on the external envelope of spike (S) glycoproteins which are responsible for entry into the host's cells (humans). This entry depends on the link between the S1 unit of the spike protein and a cellular receptor which facilitates the attachment of the virus to the surface of the target cells. (Fig. 1)

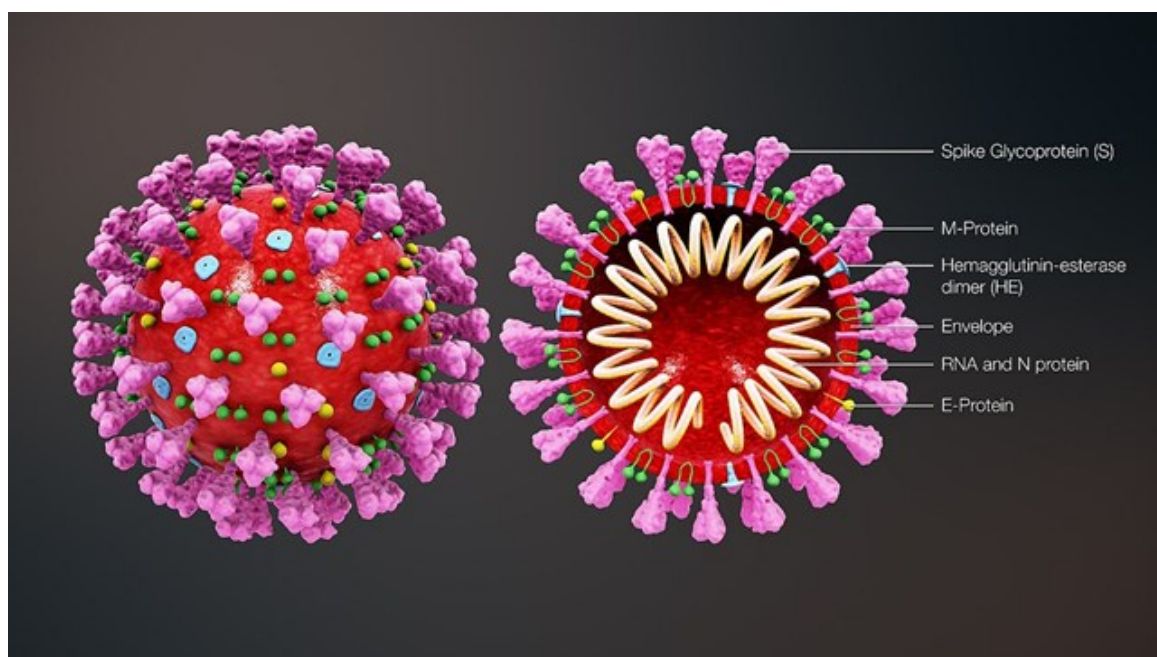


***Figure 1. Sars-CoV-2 structure***

In particular, it has been demonstrated that the virus uses the angiotensin-converting enzyme 2 (ACE2) as an entry receptor and the Transmembrane Serine Protease-2 (TMPRSS2) for the activation of the S protein (3). (Fig. 2).

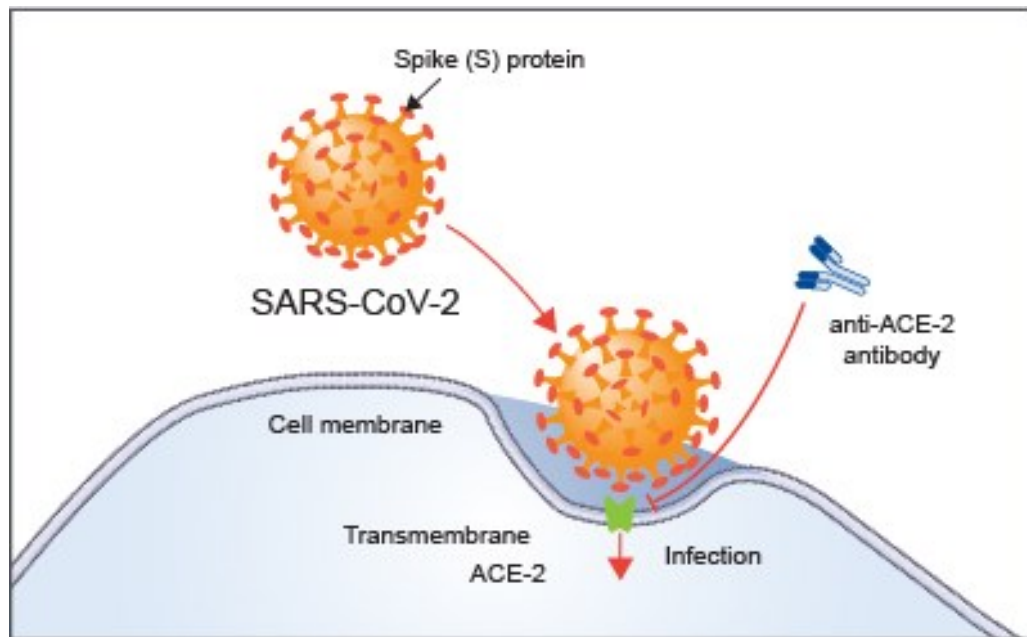


**Figure 2.** Mechanism of entry of SARS-CoV-2 through the ACE-2 receptor.

ACE2 is a homolog of ACE and plays a key role in balancing the responses caused by ACE. ACE is a Zn and chloride-dependent metallopeptidase, produced by the endothelial cells of the blood vessels of all organs, but in particular by the lung, and is responsible for the metabolism of important biologically active peptides, called Angiotensin I and Bradykinin. In particular, it catalyzes the transformation of Angiotensin I into Angiotensin II, thus intervening in the regulation of the Renin-Angiotensin-Aldosterone system. Angiotensin II is a powerful vasoconstrictor peptide: it causes an increase in peripheral vascular resistance with a consequent increase in blood pressure but also secretion of aldosterone with a consequent increase in cardiac output. There are two types of ACE: ACE1 and ACE2 (4).

The ACE2 enzyme, which degrades angiotensin II into angiotensin-(1-7), represents an entry gate for viruses of the Coronavirus family, such as SARS-CoV-2, and since this degradation occurs in a particular way when blood passes into the lungs, it has been hypothesized that greater expression of ACE2 leads to an exacerbation of the respiratory symptoms of SARS-CoV-2 infection. (5) (Fig. 3 and Fig. 4).

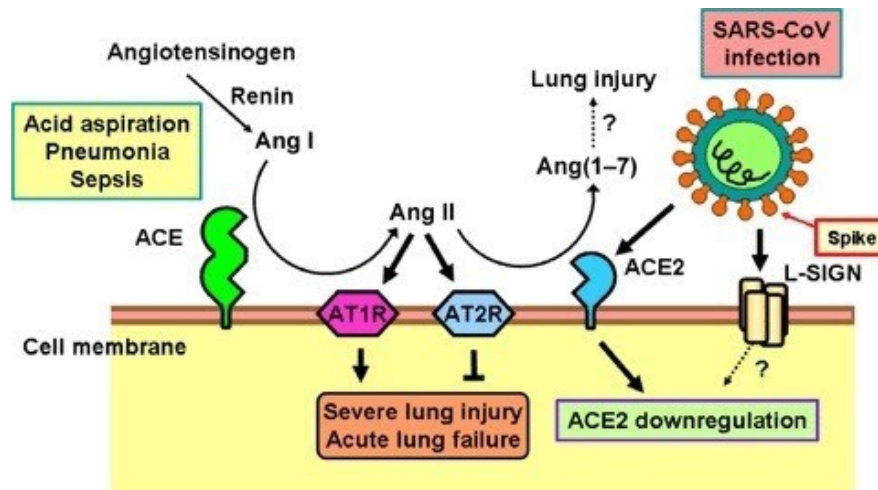


**Figure 3.** The ACE2 enzyme, which degrades angiotensin II into angiotensin-(1-7), represents an entry gate for viruses of the Coronavirus family.

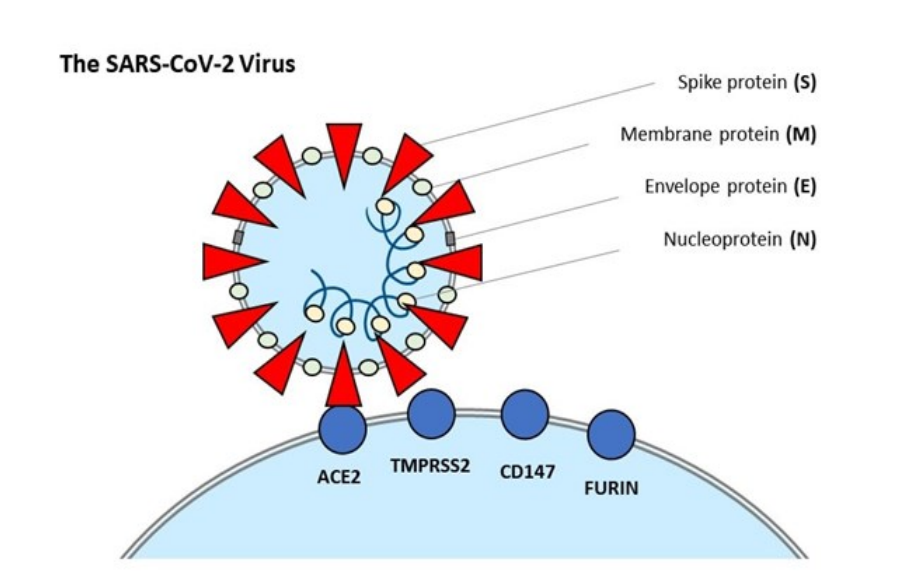


**Figure 4.** Different docking points of SARS-CoV-2 at the ACE-2 receptor

In the most serious cases, in fact, SARS-CoV-2 infection can cause acute inflammation in the lung tissues, causing interstitial pneumonia, in which there is a reduction in gas exchange at the level of the alveoli. In conditions of acute hypoxia, free radicals (ROS) are formed and therefore a consequent inflammatory state due to a reduction in oxygen supply (alteration of the vessel wall starting from the endothelium, cardiac alteration) (6).

This virus, through the ACE2 receptors, enters the organism, forcing the host's cells to produce proteins useful for replication. This initial process is responsible for the strong inflammation with consequent production of free radicals, alterations in the functionality of the pulmonary alveoli with a consequent alteration of the structure of the vessels and therefore edema. This is the reason why forced oxygen ventilation becomes necessary to remove the hypoxic state. Therefore, by reducing the inflammatory state it is possible to avoid acute respiratory crises.

One of the endogenous mediators of inflammation is IL-6, therefore its "reduction" inhibition could lead to an improvement in lung function. An important role is also played by PDEs (phosphodiesterases), a family of enzymes that metabolize cAMP and cGMP. In inflammatory cells (such as neutrophils, T lymphocytes and macrophages), cAMP interferes with the expression of pro-inflammatory mediators (e.g. TNF-alpha) and is therefore also an anti-inflammatory agent. cAMP causes relaxation of the smooth muscles of the airways, resulting in bronchodilation. One of the PDEs, PDE 4, is particularly present in the lungs and in inflamed cells. Therefore, the inhibition of PDE-4 in this case would induce an increase in cAMP and prolongation of the anti-inflammatory effect with a consequent bronchodilator effect. In fact, it is known that the inhibition of PDE-4 is useful for the treatment of COPD and also for asthma. PDE4 is divided into four sub-classes: A, B, C and D. The B form is the one most present at the level of the immune system and the respiratory system, therefore, it will be the one on which we will carry out our studies.

In Figure 5, the therapeutic effects of PDE inhibitors are reported.



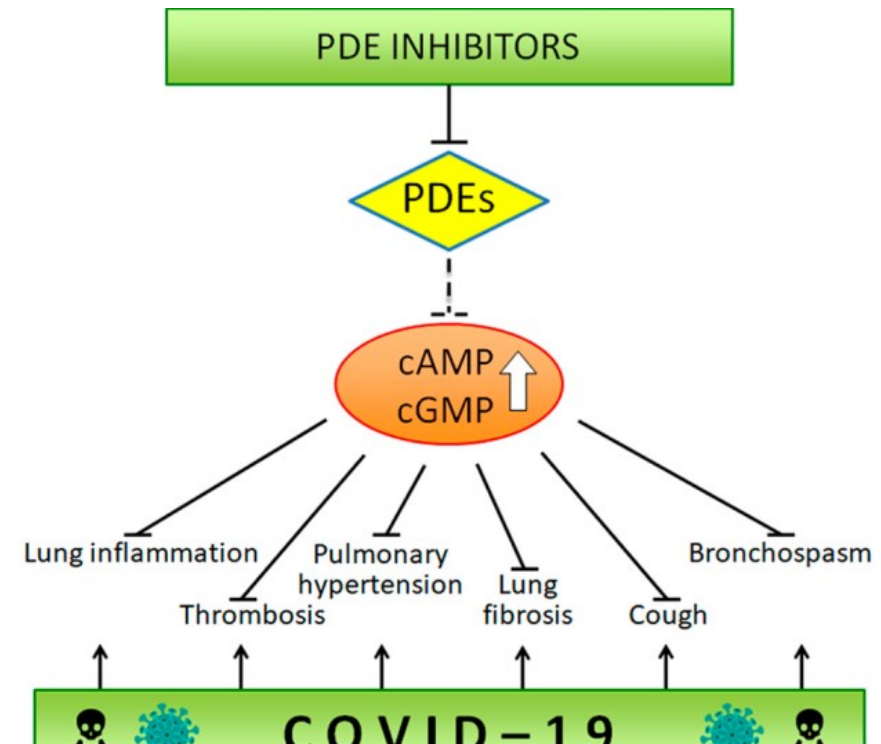


*Figure 5. Possible therapeutic effects of PDE inhibitors.*

Given the multiplicity of factors involved and responsible for the COVID-19 disease, as well as for other viral infections (such as human immunodeficiency virus HIV, human hepatitis C virus-HCV, hepatitis B virus-VBH), its inhibition could represent a multitarget and multidrug antiviral therapeutic strategy that includes a pharmacological treatment supported by a rationale that involves the use of multiple drugs in combination, such as inhibitors of the entry of the virus into the host cell, is therefore advantageous; blockade of PDE4-B; inactivation of inflammatory processes in the respiratory tract.(7,8).

Our research project involves:

- a molecular docking study on multiple classes of molecules and on selected targets involved, in particular the targets will be: PDE4-B; the Spike protein; the ACE2 receptor.
- Subsequently, those molecules that have given a satisfactory result in the theoretical study will be synthesized.

- For all synthesized molecules, *in vitro* studies on the virus and cytotoxicity studies on human cells will be performed.

# **CHAPTER 1 – SARS-CoV-2 Infection and the Global Therapeutic Scenario**

## **1.1. The COVID-19 Pandemic**

In December 2019, a cluster of pneumonia cases of unknown etiology emerged in the Chinese city of Wuhan (9). Soon after, analyses of the patient's lung fluid, blood, and throat swab reconducted this outbreak to a newly identified virus, tentatively named 2019-new coronavirus (2019-nCoV) (10). Phylogenetic analyses performed on viral genomes isolated from patients' samples revealed a close relationship between the new virus with several bat coronaviruses isolated in China (>90%). A lower degree of similarity was also found with SARS-CoV (80%) and MERS-CoV (50%), the causative agents of two recent coronavirus-related epidemics (11).

The striking similarity between the SARS-CoV-2 genome and several bat coronaviruses led to the hypothesis that bats could be the animal reservoir for SARS-CoV-2, with pangolins or other mammals acting as the intermediate host before human transmission (12). The assumption that bats could be the animal reservoir of SARS-CoV-2 was further reaffirmed at a later stage by the work of Temmam et al., which identified in the caverns of North Laos a series of bat coronaviruses that share a high level of sequence similarity (96%) with the SARS-CoV-2 genome (13).

From a clinical perspective, the spectrum of COVID-19 manifestation is broad, ranging from asymptomatic infections to severe viral pneumonia with respiratory failure and even death (14). The most common symptoms, similar to influenza, are related to mild upper respiratory tract affection, such as fever, cough, myalgia, and headache (15). Less common but still relevant ones include gastrointestinal manifestations, such as diarrhea, more severe respiratory illnesses, such as dyspnea, and multi-organ failure (16).

The long incubation time compared to similar infections (17), the capability of asymptomatic (18) or paucisymptomatic (19) patients to transmit the virus even before the eventual symptoms' manifestation, and the aerial transmission modality (20,21) all concurred to determine a higher transmissibility index (estimated between 2.5 and 3.0) for the SARS-CoV-2 virus, compared to similar viral infections (22). These factors contributed to the rapid spread of SARS-CoV-2 worldwide, resulting in more than 650 million cases and more than 6.5 million deaths globally (23).

In the first stages of the COVID-19 pandemic, extraordinary sanitary measures, such as physical and social distancing, wearing face masks and eye protection devices (24,25) were adopted to prevent the collapse of the public healthcare system (26), due to the unbalance between the high demand and the low availability of critical supplies (27,28). Although this short-term plan has proven helpful in gaining time (29,30), more sustainable and long-term oriented strategies were needed to better cope with the socio-economic (31) and psychological (32,33) consequences of the pandemic, other than ensuring a fair and efficient resource management (34).

## 1.2. Drugs Used in SARS-CoV-2 Infection

Considering that bringing a brand-new drug on the market is usually a very long and expensive process (35), the so-called "drug repurposing" was the first approach to finding suitable therapeutic options for COVID-19 patients (36,37). This strategy extends the applicability domain of already marketed drugs for treating diseases other than the one it was conceived for (38). This approach is appealing because it involves using de-risked compounds, with potentially lower overall development costs and shorter development timelines (39). Unfortunately, despite all the promising premises (40), this approach was largely unsuccessful (41). Indeed, several investigated drugs showed little to no efficacy in randomized clinical trials (42). The few successful cases were primarily symptomatic treatments, mostly limited to hospital usage for the most severe cases due to the therapy's high costs or route of administration (43).

The initial failure of the drug repurposing strategy against COVID-19 can be mostly reconducted to the very first stages of the pandemic, where few clinical pieces of evidence were available for the rational elaboration of therapy plans. For example, the combination of HIV protease inhibitors Lopinavir and Ritonavir was examined (44), despite a suboptimal predicted recognition pattern towards the SARS-CoV-2 main protease (Mpro) compared to other compounds of the same class. Another example is the combined use of an antimalaria drug (hydroxychloroquine) and an antibiotic (azithromycin) despite no clear indication of the possible mechanism of action (45,46).

With more and more clinical observations becoming available, more fine-tuned treatments, especially symptomatologic ones, were adopted. This is the case, for example, of corticosteroids such as dexamethasone (47), employed to tame the inflammatory response associated with severe COVID-19 cases, and low molecular weight heparins (48), used to

prevent or treat thrombo-embolic events associated caused by interference with the cardiocirculatory system.

A group of anti-arthritis drugs represents another successful example of drug repurposing to their ability to modulate the immune response (49) and cytokine storm (50) caused by severe SARS-CoV-2 infection. This family includes the monoclonal antibodies Tocilizumab and Sarilumab (51), which both inhibit Interleukin-6 (IL-6) signaling (52), Anakinra, that interferes instead with IL-1 signaling (53), and the Janus Kinase (JAK) inhibitor Baricitinib (54), alone or in conjunction with remdesivir (55), with the latest representing maybe the most successful example of drug repurposing against COVID-19 being the first approved drug against this illness (56-59).

Originally designed against Ebola Virus, remdesivir is a nucleotide analog prodrug that acts as a viral polymerase inhibitor (60) and is efficient in shortening the recovery time in hospitalized adult patients affected by COVID-19 (61,62). Unfortunately, as previously mentioned, remdesivir and the other repurposed drugs need parenteral administration, thereby limiting their massive-scale adoption as pharmacological treatments against COVID-19 (63).

### 1.3. Convalescent Plasma and Monoclonal Antibodies

With the first round of spontaneously healed patients, doctors started flanking standard treatment with the use of convalescent plasma (CP), *i.e.* the plasma derived from recently recovered donors with a sufficiently high neutralizing antibody titer (64,65). A similar protocol was previously adopted to face Ebola (66) and MERS (67) outbreaks, justifying its emergency use in the first stages of the COVID-19 pandemic. Unfortunately, despite promising observational data from the first studies performed on small-size patients' cohorts, more thorough investigations from more extensive clinical trials demonstrated the inefficacy of this treatment, leading to its dismissal from routine clinical practices. Despite this failure, CP inspired the design of safer and more targeted immunological treatments in the form of monoclonal antibodies (mAbs). Since the beginning of the pandemic, several mAbs directed against COVID-19 have been developed, with some obtaining approval from regulatory agencies. Multiple of these mAbs are often used in conjunction to combine their neutralizing power and boost their therapeutic efficiency, exploiting their ability to bind at different epitopes (68,69). The list of approved ones contains the therapeutic combinations of casirivimab and imdevimab (Regeneron/Roche), redanvimab (Celltrion Healthcare), sotrovimab (GSK), and the combination of tixagevimab and cilgavimab. Furthermore, the association of bamlanivimab and etesevimab is nearly approved, despite the previous failure of trials investigating bamlanivimab on its own (70,71).

## 1.4. Vaccines

As seen in the case of CP and mAbs, a targeted immune response against SARS-CoV-2 can be a beneficial treatment for patients. While immunoglobulins are limited to treating ongoing infections in hospital settings due to the high costs and the parenteral administration route, a more economical and scalable approach would be instructing the human body to produce this type of response without needing external intervention. Based on this assumption and parallel to the drug repurposing approach, the industry and academia spent a consistent joint effort on developing preventive tools to avoid the infection in the first place or at least mitigate the most detrimental effects of the illness. This endeavor resulted in the quick approval by regulatory agencies of several vaccines (72,73).

Three different classes of these therapeutic entities can be recognized. The first one, related to inactivated virus vaccines, comprises the Chinese CoronaVac (Sinovac) and the Russian CoviVac. The second group is formed by adenovirus vector vaccines such as Vaxzevria/ChAdOx1-S (AstraZeneca), Sputnik V/Gam-COVID-Vac, and Jcovden/Ad26.COVS.2.S (Janssen). Finally, the third one is composed of mRNA-based vaccines, including Comirnaty/BNT162b2 (Pfizer-BioNTech) and Spikevax/mRNA-1273 (Moderna) (74-76).

Despite the poor performances of the first class of vaccines, several independent studies have asserted worldwide the efficacy of vaccination campaigns based on the other two types of vaccines, particularly in the case of mRNA-based ones (77-80).



## 1.5. Viral Variants

Due to its exposition on the external surface of the SARS-CoV-2 membrane and its pivotal role in the virus' ability to infect host cells, the spike protein is often subjected to mutations that alter the virus's infectivity and antigenicity (81,82). Therefore, since the spreading of the original viral strain (Wuhan-Hu-1) began, several viral variants appeared on the scene (83), particularly in the Third-world Nations where collective sanitary practices like social and physical distancing (84) or wearing face masks in public places 18 were hardly implementable (85). The insurgence of novel viral strains with different susceptibility to the protective effect of vaccines (86) demands a periodical update of their original formulations coupled with multiple booster shots to maintain their efficacy (87), thus hampering the management of the pandemic based on massive vaccination of the world population (88,89).

Among the large pool of SARS-CoV-2 mutations, some gathered the scientific community's attention due to their increased fitness, gaining the "variant of concern" (VOC) status (90,91). The first SARS-CoV-2 VOC was the B.1.1.7 variant, more commonly referred to as the "Alpha" or "English" variant due to being first identified in November 2020 in the Kent region of the United Kingdom (92,93). Despite worries about the higher transmissibility compared to other circulating variants at the time (94,95), clinical studies appointed how mAbs, CP, and especially vaccines, were still able to confer protection against B.1.1.7.108–110, containing its impact on the sanitary system (96).

Unfortunately, soon after the emergence of the Alpha variant, a more threatening VOC arose. The B.1.617.2 variant, commonly known as the "Delta" or "Indian" variant due to being first identified in India in late 2020, quickly overthrew the B.1.1.7 one thanks to its strikingly increased transmissibility (97). The advent of the Delta variant was associated with the first signs of reduced protection provided by mAbs, CP, and most importantly,

vaccines (98–100), thanks to its increased immune system evasion capability, posing a heavier workload on the sanitary system (111,112).

The latest hallmark in the history of SARS-CoV-2 variants is represented by the B.1.1.529 variant, first detected in South Africa and more often recalled as the Omicron variant (113). The combination of increased transmissibility (114) and immune system evasion (115) conferred this variant a net selective advantage in bypassing the protection provided by the complete primary vaccination cycle and a variety of clinically utilized mAbs (116–118) compared to other circulating strains. The ground-breaking impact the Omicron variant had on the worldwide spread of SARS-CoV-2 even led to the introduction of the "booster dose" to compensate for the reduced coverage of the primary vaccine cycle (119). Lately, several subvariants germinated from the original Omicron strain (also labeled as BA.1), namely BA.2, BA.3, BA.4, and BA.5<sup>124–126</sup>. Although different studies indicated how the first identified Omicron subvariants (BA.2 and BA.3) were similarly susceptible to existing treatments despite their increased transmissibility, it also emerged how the most recently identified ones (BA.4 and BA.5) are significantly more efficient in evading the immune response. These findings indicate that SARS-CoV-2 continued to evolve by increasing its immune-evasion capability rather than counting on sheer higher transmissibility, sustaining the virus spread even in populations with high vaccination frequency and recovery rates (120).

## 1.6. Spike Protein

The ability of the SARS-CoV-2 virus to infect human cells heavily depends on a surface glycoprotein known as the S/spike protein (121), named after its peculiar shape (122). For this reason, both mRNA vaccines and mAbs are designed to target this protein and prevent the virus entrance within the cell, thereby limiting its replication (123).

Concerning these, although different pathways for SARS-CoV-2 cell entry are possible (124,125) the principal and better-characterized one involves binding to the human ACE2 receptor (hACE2) (126), a membrane-anchored metallopeptidase that is abundantly present in various districts of the human body, from the vascular endothelium to the epithelia of lungs and small intestine (127). On its own, host cell receptor binding is not sufficient to ensure entrance within host cells. Priming and activating the S protein by host proteases is required to enhance its cell-cell and virus-cell fusion processes and increase viral shielding from neutralizing antibodies (128,129). The list of priming proteases included, but is not limited to, TMPRSS2, a transmembrane serine protease that is often co-expressed with ACE2 in SARS-CoV-2 target cells, Furin and cathepsin B/L, (130,131). The priming process entails the exposure of a lipophilic fusion peptide (FP), which penetrates the host cell membrane triggering the viral fusion thanks to its strong membrane-perturbing capacities (132,133)

From a structural perspective, the spike is a trimeric transmembrane glycoprotein composed of 1273 amino acids organized in two main subunits, S1 and S2, and several functional domains.

The S1 subunit comprises two main domains, specifically the N-terminal and C-terminal domains (NTD and CTD, respectively), which are both involved in the binding to host cell receptors (134). The CTD contains the receptor-binding domain (RBD, residues 319–541),

consisting of two motifs. Firstly, a core structure formed by a twisted five-stranded anti-parallel  $\beta$  sheet ( $\beta 1$ ,  $\beta 2$ ,  $\beta 3$ ,  $\beta 4$ , and  $\beta 7$ ), with three short helices ( $\alpha 1$ ,  $\alpha 2$ , and  $\alpha 3$ ). Secondly, an extended loop (receptor binding motif, RBM), formed by a two-stranded  $\beta$  sheet ( $\beta 5$  and  $\beta 6$ ), lying at one edge of the core and containing most of the residues involved in binding to hACE2 (135).

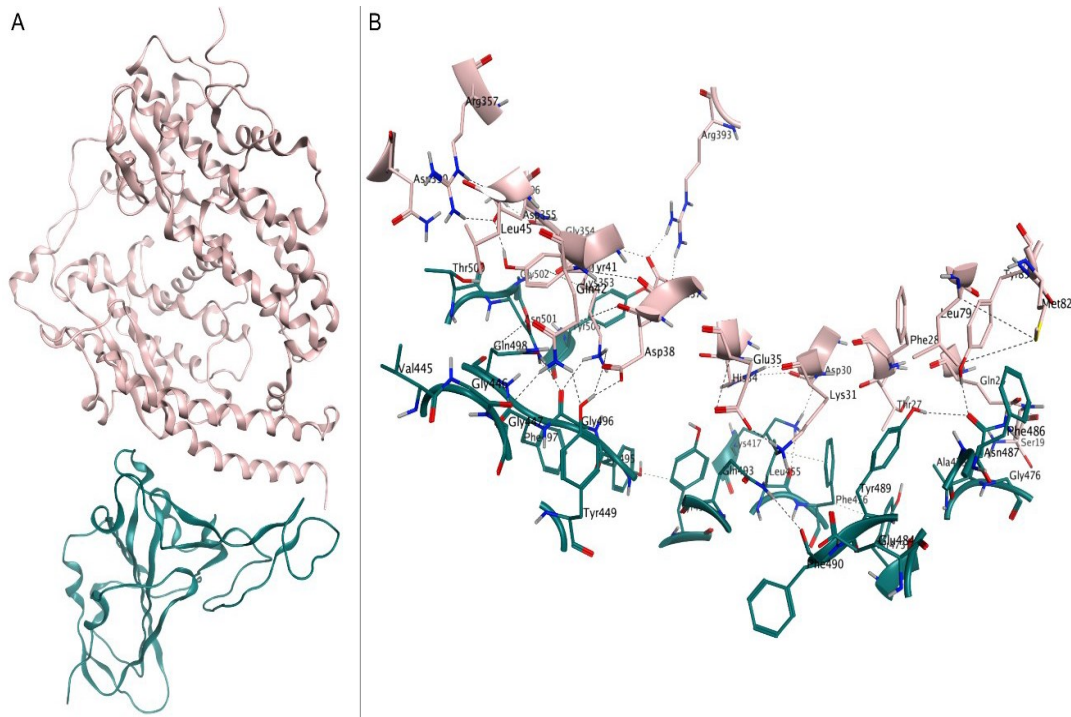


**Figure 6.** (A) Crystal structure of spike RBD (pink) in complex with hACE2 (teal), deposited in the Protein Data Bank with accession code 6M0J. (B) Close-up view of interface contacts between the spike RBD and hACE2: hydrogen bonds are represented as black dashed lines.

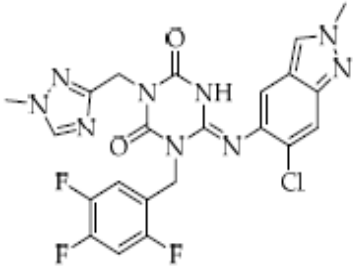
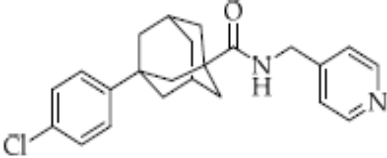
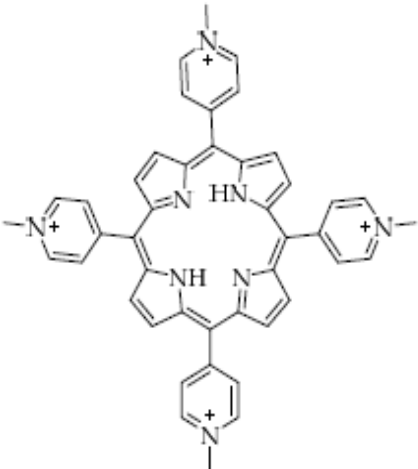
The S2 subdomain has significant roles in spike protein trimerization and in mediating the virion entry into the host cell once the molecular contacts have been established (136). It is formed by relevant subdomains such as the transmembrane domain (TD) (residues 1296–1317), which exerts both the spike anchoring to the outer side of the viral membrane and the maintenance of the trimeric quaternary structure and a cytoplasm domain (CD) (residues 1318–1353), which mediates viral assembly and cell-cell fusion. Furthermore, the previously mentioned fusion peptide, a cleavage S2' site (residues 815/816), and two heptad-repeat domains (HR1/HR2) (residues 984–1104/1246–1295) are also part of S2 (137).

## 1.7. Recent Studies for New Drugs

In view of the ongoing mutation of SARS-CoV-2 (such as Omicron), new clinical studies have been addressed to small-molecule anti-CoV drugs, considering the convenience and flexibility of oral administration and the large production capacity. These are summarized in Table 1. Some clinical advances in the development of small-molecule drugs targeting SARS-CoV-2 3CLpro have been reported by Hu et al. (138). The noncovalent, reversible oral nonpeptidic SARS-CoV-2 3CL protease inhibitor clinical candidate, namely S-217622 developed by Shionogi, has been deeply studied (139). This compound was discovered via virtual and biological screening of an in-house compound library, and optimization of the hit compound using a structure-based drug design strategy (140). It is under evaluation in a phase III clinical trial (NCT05305547) and is a prospective oral therapeutic option for COVID-19. Moreover, new viral and cellular pathways are currently being investigated as potential targets to develop effective therapy to stop the pandemic (141).

Recently, the nanoligomer treatment SBCoV207, which has been already validated for its ability in mitigating uncontrolled immune response in SARS-CoV-2 infection (142), has shown a high bioavailability and biodistribution to the lungs and produced no toxicity in mice at 10 mg/kg, when administered via intranasal, intraperitoneal, or intravenous routes (143). Opaganib (aka ABC294640), a drug targeting the sphingolipid metabolism and used for the treatment of inflammatory diseases, also exhibited an antiviral activity towards different viruses, including SARS-CoV-2. Particularly, opaganib reduced the mortality of patients with moderately severe COVID-19 by about 62%, due to its ability to suppress SARS-CoV-2 infection and replication by inhibiting three enzymes in sphingolipid metabolism: sphingosine kinase-2, dihydroceramide desaturase and glucosylceramide synthase. Thus, this drug may represent a safe alternative to remdesivir and dexamethasone

with both antiviral and anti-inflammatory properties (144). Interestingly, G-quadruplexes specific ligands, namely 5,10,15,20-tetrakis-(*N*-methyl-4-pyridyl) porphine (TMPyP4), showed better antiviral effects than remdesivir on the Vero E6 cells, Syrian hamster and hACE2 transgenic mouse model of SARS-CoV-2 infection, with no significant toxicity (145). Most importantly, this study provided an alternative strategy for COVID-19 treatment by targeting the secondary genomic structures of SARS-CoV-2, paving the way to the rational design and synthesis of new safer agents.

Structure	Name	Activity
	S-217622	SARS-CoV-2 3CL protease inhibitor
	Opaganib	Sphingosine kinase-2, dihydroceramide desaturase and glucosylceramide synthase inhibitor
	5,10,15,20-tetrakis-( <i>N</i> -methyl-4-pyridyl)porphine (TMPyP4)	G-quadruplexes specific ligand

**Table 1.** New drugs for the treatment of COVID-19 (146).

## 1.8. Potential Targets of Interest

Although targeting the SARS-CoV-2 main protease was successful in individuating several clinical candidate drugs, and even led to the first approval of COVID-19 specifically designed drugs, other drug discovery campaigns aimed at different viral targets are needed for therapy diversification, potential combined and synergic treatment, and resistance prevention (147,148).

Altogether, the SARS-CoV-2 genome encodes four major structural proteins, including nucleocapsid (N), membrane (M), envelope (E), and the spike as mentioned earlier (S), plus 16 nonstructural proteins, encompassing the previously mentioned main protease (149). Although Mpro plays a pivotal role in processing the SARS-CoV-2 viral polyproteins, it is not the only component of the functional replicase complex that is required for the viral spread process (150). Alongside it, a secondary but still relevant enzyme operates, namely the papain-like protease (PLpro, the catalytic domain of protein nsp3) (151). Despite being a cysteine protease like Mpro, PLpro exerts its enzymatic functions through a catalytic triad composed of Cys111, His272, and Asp286 (152). Further, PLpro processes peptide bonds located at the C-terminal end of LXGG motifs (153). Functionally speaking, this 343 residues segment which is part of the multidomain nsp3 protein is responsible for cleaving the SARS-CoV-2 polyproteins at three different sites, resulting in the liberation of nsp1, nsp2, and nsp3 proteins (154). Moreover, PLpro is also responsible for cleaving post-translational modifications on known regulators of host innate immune response (155).

As demonstrated by the approval of Remdesivir by regulatory agencies, another valuable target for the development of COVID-19 drugs is represented by the RNA-dependent RNA polymerase (RdRp)<sup>49</sup>. This complex machinery comprises four subunits, including one nsp12, responsible for the catalytic activity of the assembly, one nsp7, and two nsp8, with the latest two acting as cofactors (156). The assembled holoenzyme presides RNA

replication, a process that results in the formation of nine subgenomic RNAs (157). The active site of nsp12 resides in its C-terminal RdRp domain and includes residues spanning from Thr611 to Met626, which are involved in binding one turn of double-stranded RNA, while residues D760 and D761 are required for recognition of the 3' end and essential for RNA synthesis (158,159). Remdesivir binds within the active site, forming direct contact with residues K545, R553, D623, S682, T687, N691, S759, D760, and D761 and blocking the catalytic machinery by delaying the chain termination process (160,161).

During the RNA synthesis process, the RdRp interoperates also with nsp13 (helicase) (162), an enzyme involved in unwinding the RNA secondary structure of the 5' untranslated section of viral genome (163) to increase the efficiency of the copy process (164,165). From a structural perspective, the nsp13 is a 596 residue, triangular pyramid-shaped helicase, which exploits its function thanks to the energy provided by its NTPase domain composed of six conserved residues (K288, S289, D374, E375, Q404, R567) (166). Adding to its helicase activity, the nsp13 active site also exerts RNA 5' triphosphatase activity, further highlighting its importance in the maturation process of the viral mRNA (167). The 5' end of the newly synthesized mRNA is then subjected to post-translational modifications to boost both its stability (preventing cleavage from exonucleases), protein translation, and viral immune escape (168). This activity is sequentially carried out by two S-adenosyl-L-methionine-dependent methyltransferases, namely nsp14 and nsp16 (169).

Specifically, the 527 residue nsp14 encompasses both a proofreading exoribonuclease (ExoN) and an N7-methyltransferase enzymatic activity (170). Furthermore, it has recently been suggested that it could encompass also a third, essential function for the viral replication cycle, based on the fact that SARS-CoV-2 ExoN knockout mutants are nonviable despite the 95% sequence identity with SARS-CoV (171) and the conservation of important active site amino acids including both the cap-binding residues (N306, C309, R310, W385, N386,



N422, and F426) and the S-adenosyl methionine (SAM) binding residues (D352, Q354, F367, Y368, and W385) (172,173).

After its cleavage by the Mpro, evidence suggests that it forms a binary complex with nsp10 which cooperatively exerts the proofreading activity on fresh RNAs produced by the RdRp machinery (174,175). Although the binary complex theory is the most prominent one, an alternative hypothesis based on the formation of a ternary nsp10-nsp14-nsp16 has been proposed due to the flexibility of the lid subdomain of nsp14 and the fact that nsp10 also forms a heterocomplex with nsp16.

Particularly, the nsp16-nsp10 heterodimer is responsible for the 2' O-methyltransferase activity that is required to complete the cap-0 → cap-1 conversion of mRNA that is initiated by nsp14. While the catalytic activity entirely resides on nsp16, nsp10 portrays a support role, aiding the recruitment of both the m<sup>7</sup>GppA-RNA substrate (which happens at a binding site defined by residues K24, C25, L27, Y30, K46, Y132, K137, K170, T172, E173, H174, S201, and S202) and the SAM cofactor (which binds in a pocket defined by N43, G71, G73, G81, D99, D114, C115, D130, and M131), thus enhancing nsp16's catalytic activity (176,177).

Lastly, another essential target for coronavirus biology is represented by nsp15, a uridine-specific endoribonuclease (NendoU) (178). The active form of this enzyme is a dimer of trimers, with each monomer composed of 345 residues organized in three different domains: N-terminal, middle, and C-terminal NendoU, where the catalytic activity resides (179). The active site contains six conserved residues: His250, His250, and Lys290, which compose the catalytic triad, Thr341, Tyr343, and Ser294, with the latest associated with selectivity in substrate recognition (180). Due to their localization within the hexamer, cooperativity or anti-cooperativity between different binding sites is possible (181). Nsp15

enzymatic activity involves the cleavage of both single- and double-stranded RNA at uridine sites producing 2',3'-cyclic phosphodiester, and 5'-hydroxyl termini (182).

Functionally speaking, Nsp15 seems to directly participate in viral replication through interference with the innate immune response. Indeed, to evade host pattern recognition receptor MDA5 responsible for activating the host defenses, the Nsp15 cleaves the 5'-polyuridine tracts in (-) sense viral RNAs, though it has also been suggested that Nsp15 degrades viral RNA to hide it from the host defenses (183-185).

## CHAPTER 2 – Aim of the Research

SARS-CoV-2, responsible for the COVID-19 infection, is an RNA virus belonging to the Coronavirus (CoV) family. This virus causes severe inflammation of the respiratory tract epithelium and can lead to the death of the patient who is affected. There are currently no valid drug therapies. It appears under the electron microscope as a crown (hence the name) due to the presence of spike glycoproteins (S) on its outer envelope which facilitate entry into target cells. This input depends on the binding of the S1 unit of the protein S to a cell receptor, which facilitates the attachment of the virus to the surface of the target cells. In particular, it engages the ACE2 as an entry receptor and the serine protease TMPRSS2 for the activation of protein S. The ACE2 receptor is an important protein that regulates the vasoconstriction processes of the arteries. This membrane protein is present on the cells of the epithelium of the lungs, protecting them from damage that can be caused by infections and inflammation, and is also expressed in heart, kidney and intestinal tissues. In severe cases, SARS-CoV-2 infection can cause acute inflammation in the lung tissues causing interstitial pneumonia, in which there is a reduction in gas exchange in the alveoli.

As well as for other viral infections (eg HIV, HCV, HBV), a multitarget and multidrug antiviral therapeutic strategy that includes a drug treatment supported by a rationale involving the use of several drugs in combination could be advantageous.

This could be achieved:

- 1 preventing the binding with the ACE2 receptor;
- 2 reducing the inflammation caused by SARS-CoV-2 and which seems to be involved in the subsequent complication of a vasculitic nature that affects multiple areas of the body;
- 3 blocking the deposit of fibrin on the alveoli.

Therefore, we proposed to create a "multitarget and multidrug" system with molecules made by total synthesis in order to be able to counteract the action of the virus on several fronts and at various levels. For the realization of this research project, we will take care of the various steps, from molecular modeling, to synthesis, to *in vitro* study, also making use of experts in various sectors (virologists, pathologists, pulmonologists, intensivists, internists) and experts in phylogenetic analysis.

The phylogenetic analysis will be used for a first screening of SARS-CoV-2 sequences to check if there are phylogenetic clusters that detect genetic differences between the sequences. Furthermore, viral genome sequences will be analyzed to identify mutations under positive selection and recombination events.

Recently the research group that will coordinate this project has already begun to work on the idea proposed here by identifying a series of molecules, some of which have already been subjected to computational calculations.

The whole study was take place in three phases (in the three years of the doctorate), obviously interconnected, as phase 2 was start immediately at the end of phase 1 for each class of compounds, as well as phase 3 was start for each molecule just completed. synthesis and characterization. Obviously for some molecules already synthesized we could start immediately from Phase 3, while for others already identified we was start from phase 2.

In general, the three phases in which the PhD project was be divided are the following:

**Phase I.** Molecular Docking study on selected targets involved (in particular: spike proteins, ACE2 receptor, iPDE4B).

An idea, certainly to be developed, stems from the study of the chemical-pharmaceutical properties of Gabesate, an *in vivo* inhibitor of serine proteases and characterized by a guanidine grouping. This drug, has anticoagulant properties, is an inhibitor of inflammatory cytokines (TNF-alpha and IL-6). TNF-alpha is a cytokine produced primarily by the immune

system and is the first to be produced following infections. Many derivatives of this class possess inhibitory activity against phosphodiesterases and in particular against PDE4. PDE4 is predominant in lung tissues, following its inhibition in inflammatory cells, there is an increase in AMPc, and this generates an anti-inflammatory action producing a bronchodilator effect. SARS-CoV-2 contains an extra "piece" in its genome, a sequence of amino acids that is actually well known to virologists because it is common to some of the most devastating viruses that affect humans, even if for the rest they are completely different parasites among them: Ebola, HIV, highly pathogenic strains of avian flu, Zika and even another coronavirus, MERS, which does not use the ACE2 receptor. Neuropilin is found on the outside of our cells and binds to a lateral tract of the spike, the virus's hook protein. Instead, ACE2 "sticks" with the top of the viral protein. If the receptors are both present, as happens in some cells of the respiratory tract, the infectious power of the coronavirus is expressed to the maximum degree ".

This first modeling phase will allow you to design and identify the lead compounds.

**Phase II:** Synthesis, for each class, of the lead molecule, physico-chemical characterization and stability tests.

It should be emphasized that for all the types of molecules proposed, there are known synthetic pathways, developed by the same researchers involved in the project, for similar molecules. This obviously will allow the objectives identified in the modeling phase to be achieved in a short time.

**Phase III:** Biological testing of selected compounds in vitro on the virus and cytotoxicity studies on uninfected human cells.

The active molecules will represent the prototype leads to investigate (in the second funding phase) the mechanisms and molecular targets involved and from which to start for the design and synthesis of even more effective analogues. Toxicity studies may also be performed *ex vivo*.

## **CHAPTER 3 – Potential PDE4B Inhibitors against SARS-CoV-2 Infection**

### **3.1. Introduction**

SARS-CoV-2 is a member of the Coronavirus family responsible of the worldwide pandemic of human respiratory illness COVID-19 (186). Several studies are addressed to find new drug targets and vaccines to curb this disease (187-191). Among the different involved targets, cyclic nucleotide phosphodiesterases (PDEs) are being investigated, a large superfamily of enzymes which play a major role in intracellular signaling by controlling tissue cAMP (cyclic 3',5'-AMP) and cGMP (cyclic 3',5'-GMP) levels in response to receptor activation. Among the 11 subtypes of PDE family, PDE4 is the principal cAMP-metabolizing enzyme found in the immune and inflammatory cells. The inhibition of PDE4 may induce an increase in cAMP (192,193) and prolongation of the anti-inflammatory effect with a consequent bronchodilator effect. Thus, PDE4 inhibitors have been proven as anti-inflammatory agents against different pulmonary disorders through inhibition of the release of inflammatory signals and cytokines (194). This inhibition has been addressed for diverse diseases (195), including inflammatory diseases (196), the topical treatment of psoriasis (197) and atopic dermatitis (198), cancer (199), inflammatory bowel diseases (200,201), neurological disorders (202), diabetic nephropathy (203), and pulmonary dysfunctions in COVID-19, such as chronic obstructive pulmonary disease (COPD) (204,205).

Several studies are being carried out on PDE4 inhibitors in order to understand their mechanism of action. Our study was focused on rolipram and piclamilast (RP 73401) (Fig. 7) (206,207). Rolipram (4-(3-cyclopentyloxy-4-methoxyphenyl)-2-pyrrolidone, A, Fig. 7) was designed as a COPD therapeutic target acting as a PDE4 inhibitor (208,209). PDE4 inhibition by piclamilast (3-cyclopentyloxy-N-(3,5-dichloropyridin-4-yl)-4-

methoxybenzamide, B, Fig. 7) was effective in preventing blast-induced long-term potentiation deficits (210). A possible mechanism of action responsible of the anti-inflammatory and immunomodulatory effects of this class of compounds has been recently suggested by Nguyen et al. (211) for tanimilast, a new potent and selective inhaled inhibitor of PDE4 in advanced clinical development for the treatment of COPD. The study was carried out in vitro on a model of dendritic cell activation by SARS-CoV-2 genomic ssRNA (SCV2-RNA). Tanimilast lowered the release of pro-inflammatory cytokines (TNF- $\alpha$  and IL-6), chemokines (CCL3, CXCL9, and CXCL10) and of Th1-polarizing cytokines (IL-12, type I IFNs).

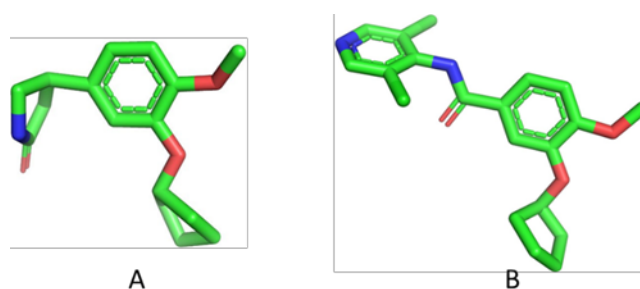


**Figure 7.** PyMOL version of rolipram (A) and piclamilast (B).

PDE4, which consists of different isoforms (212), comprises four subtypes, PDE4A, B, C, and D. Non-selective PDE4 inhibitors, which bind all four PDE4 subtypes simultaneously, produce many promising therapeutic benefits, accompanied however by unwanted side effects, principally, nausea, diarrhea, and emesis (213); they may also induce gastroparesis, as demonstrated in mice (214). Thus, the selective inhibition of a single subtype may be addressed. In particular, our study was aimed to the PDE4B subtype, that has been related to diverse activities. PDE4B inhibitors have been also suggested as promising therapeutic targets for *Pseudomonas aeruginosa*, which is a frequent cause of hospital-acquired lung infections (215) and other molecules have been designed and studied

as potential PDE4B inhibitors to reduce or block inflammatory processes of the respiratory tract (216,217). Indeed, PDE4B regulates the pro-inflammatory toll receptor–tumor necrosis factor  $\alpha$  pathway in monocytes, macrophages and microglial cells.

Interestingly, it has been demonstrated that PDE4B, which is the predominant form in the immune and respiratory systems, is involved in human respiratory illness coronavirus disease 2019 (COVID-19), the worldwide pandemic caused by severe acute respiratory syndrome coronavirus-2 (SARS-CoV-2) (218,219). Therefore, it represents molecular target for anti-inflammatory and antiviral drugs. Unfortunately to date, the development of selective PDE4B inhibitors is not easy as the amino acid sequence of the PDE4 active site is identical in all PDE4 subtypes (PDE4A-D) (221). However, recently a modeling study was carried out on PDE4B and PDE4D active cavity (222). Among the PDE4 selective inhibitors, roflumilast, which shows higher affinity to PDE4B than PDE4A, C and D, represents a potential and effective therapy for COVID-19 (223). Moreover, a PDE4B selective inhibitor, BI 1015550 has been proposed as a clinical drug candidate for the oral treatment of idiopathic pulmonary fibrosis (224). In this view, aim of our work was the design of new selective inhibitors of PDE4B as potential therapeutic agents for COVID-19 disease. Specifically, twenty-one in house molecules were examined and correlated to the structures of piclamilast and rolipram in order to seek greater possible interactions with the catalytic site of the A chain of PDE4 (225).

Recently, a modeling study was carried out on PDE4B and PDE4D active cavity (226). Piclamilast and rolipram were chosen since in the literature they are among the major PDE4 inhibitors ( $IC_{50} = 1.1$  nM and 1200 nM for piclamilast and rolipram, respectively) (227). The magnesium and zinc ions present at the catalytic site of PDE4B were taken into account for the docking study, by using AutoDock Vina software, as they could be involved in PDE4B inhibitory activity. Drug likeness predictions, i.e. physicochemical-



pharmacokinetic and ADME (absorption, distribution, metabolism, and excretion) properties, of the studied compounds have also been performed. These studies will allow us to select the best compounds to be proposed for future in depth in vitro and/or in vivo studies. We are confident that the identification of potentially active molecules could be important for the discovery and development of new drugs for COVID-19 and at the same time useful for the study of the molecular mechanisms involved in this devastating disease.

### 3.2. Rationale for Molecular Docking Studies

A molecular docking study was performed on piclamilast and rolipram in the catalytic site of PDE4B, located mainly on the A chain of PDE4B (PDB code: 1XM4) (228). AutoDock Vina was used for docking (229). The magnesium and zinc ions present at the catalytic site of PDE4B were also considered. With this study it is possible to predict the structure of the ligand-protein intermolecular complex, and to establish what in the jargon is called Pose or Binding Mode, that is the position, orientation and conformation that each individual ligand assumes on the surface of the biological receptor macromolecule. All the side chains of the flexible amino acid residues selected have been included in the flex file, that is, those side chains, present in the active site on the A chain of PDE4B in that could have a probable interaction with the ligand (Fig. 8). In particular, the selected residues are: ARG`409, ASN`235, ASN`283, ASN`395, ASP`275, ASP`346, ASP`392, CME`432, GLN`284, GLN`443, GLU`304, HIS`234, HIS`238, HIS`274, HIS`278, HIS`307, ILE`410, ILE`450, LEU`303, LEU`393, MET`347, MET`411, MET`431, PHE`414, PHE`446, SER`229, SER`236, SER`282, SER`348, SER`429, SER` 442, THR`345, THR`407, TYR`233, TYR`403, TYR`449. Also for the ligand a file with the extension .pdbqt has been created, in which its atoms have been defined; its potentials and its degrees of freedom. This last process was obviously repeated for all ligands tested.

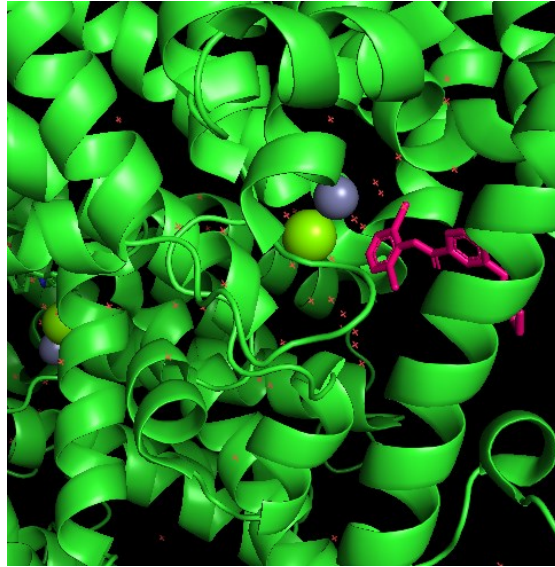


**Figure 8.** *Catalytic domain of human phosphodiesterase 4B in complex with piclamilast (in magenta).*

Piclamilast is a selective second-generation PDE4 inhibitor with important anti-inflammatory effects (229). It has been studied for its applications in the treatment of conditions such as COPD, bronchopulmonary dysplasia, and asthma. It acts through the selective inhibition of the four PDE4 isoforms (PDE4A-D), while shows no inhibition of the other PDEs (230). PDE4 isoforms are particularly important for inflammatory and immunomodulatory cells. They are the most common PDE in inflammatory cells such as mast cells, neutrophils, basophils, eosinophils, T lymphocytes, macrophages, and structural cells such as sensory nerves and epithelial cells. Inhibition of PDE4 blocks the hydrolysis of cAMP thereby increasing the levels of cAMP within the cells. cAMP suppresses the activity of immune and inflammatory cells, thus, the inhibition of PDE4 in a mouse model of induced chronic lung disease demonstrated anti-inflammatory properties, determined the reduction of pulmonary fibrin deposition and alveolar vascular loss, and prolonged survival in hyperoxia-induced neonatal lung injury. Moreover, a PDE4 inhibition study in a mouse model of allergic asthma showed that piclamilast significantly improved lung function, airway inflammation and goblet cell hyperplasia. Recently, the neuroprotective effect of piclamilast has been studied. It has been suggested that post-ischemia pharmacological

treatment with piclamilast determines an improvement of cerebral ischemia–reperfusion injury in mice (231). The docking study with piclamilast gave the following resulting poses (Table 2).

**Table 2.** Docking study with piclamilast. The average rmsd of the poses are compared with pose 1.

<b>pose</b>	<b>binding energy "affinity" (kcal/mol)</b>	<b>rmsdl.b.</b>	<b>rmsdu.b.</b>
1	-10.1	0.000	0.000
2	-9.5	0.851	1.392
3	-9.4	0.807	2.110
4	-8.4	1.023	2.553
5	-8.4	1.480	2.512
6	-8.0	1.276	2.087
7	-7.8	1.624	4.096
8	-7.8	1.734	2.126
9	-7.7	1.520	2.351

The docking results show a similar bonding energy for pose 2 and pose 3, equal to -9.5 and -9.4 kcal/mol, respectively. The nine poses obtained from the docking were compared to the pose of piclamilast obtained experimentally with PyMol.

Rolipram is a selective PDE4 inhibitor discovered and developed as a potential antidepressant drug in the early 1990s. It has been used as a prototype molecule for drug discovery and pharmaceutical research development by several companies. The study on rolipram was stopped after clinical trials showed that its therapeutic window was too narrow; it could not be used at levels high enough to be effective without causing significant gastrointestinal side effects. Nevertheless, rolipram has several activities that make it a continuing target for research (232-235). Rolipram has been used to study whether PDE4 inhibition could be useful in autoimmune diseases, Alzheimer's disease, cognitive enhancement, spinal cord injury, and respiratory diseases such as asthma and COPD (236). In this study, rolipram was used to better understand the exact level of exhaustiveness to be used to set the data when starting molecular docking. The data obtained with an

exhaustiveness of 16 are satisfactory and comparable to those obtained with piclamilast. The results of the docking study with rolipram gave the following poses (Table 3).

**Table 3.** Docking study with rolipram. The average rmsd of the poses are compared with pose 1.

pose	binding energy "affinity" (kcal/mol)	rmsdl.b.	rmsdu.b.
1	-8.4	0.000	0.000
2	-8.4	1.124	2.156
3	-8.2	1.322	3.113
4	-8.2	1.291	2.763
5	-8.1	1.355	2.998
6	-8.1	1.602	2.875
7	-7.8	1.237	1.902
8	-7.7	1.354	2.961
9	-7.5	1.458	2.124

The docking results show the same binding energy for pose 1 and pose 2, equal to -8.5 kcal/mol. The nine poses obtained from docking were compared with the data obtained experimentally by PyMol. The conformation that overlaps almost perfectly is pose 1 (Fig. 9).

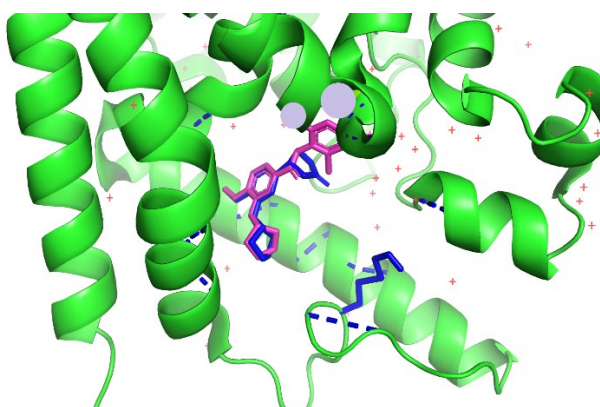


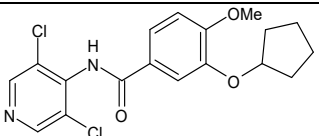
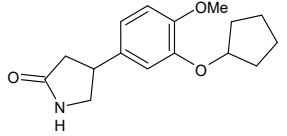
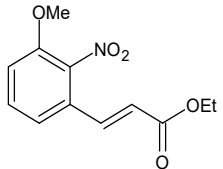
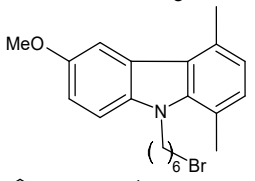
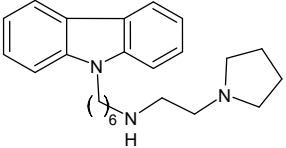
**Figure 9.** Comparison between the crystalline structure of piclamilast (in magenta), with pose 1 of the docking of rolipram (in blue). Part of the catalytic site of PDE4B with part of the flexible residues is visible in green.

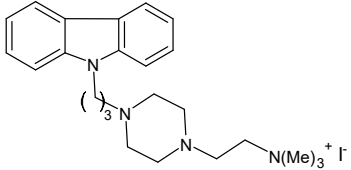
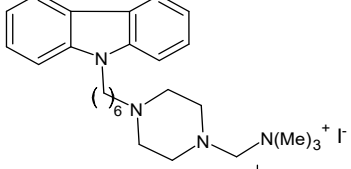
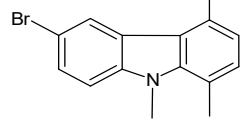
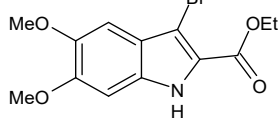
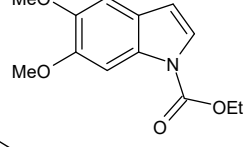
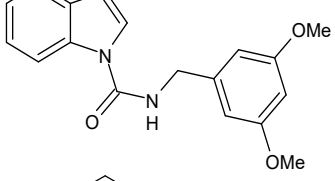
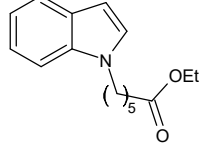
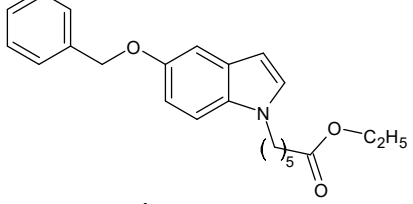
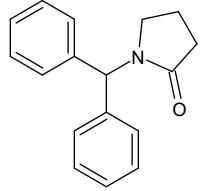
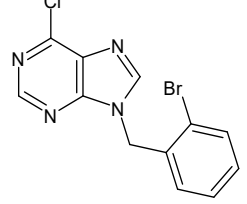
From the data obtained with different degrees of exhaustiveness (4, 8, 12, 14, 16, 20) for piclamilast and rolipram, we concluded that level 16 was the most favorable gave the

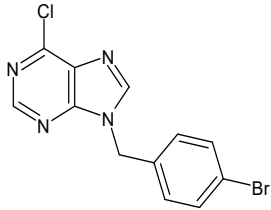
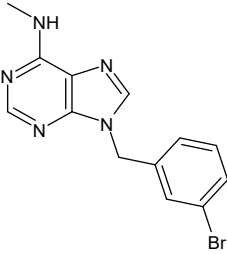
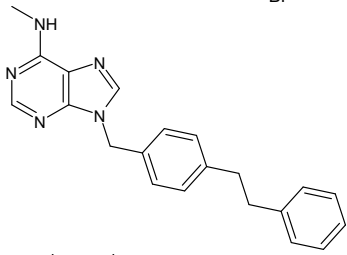
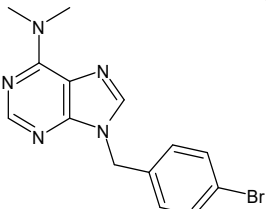
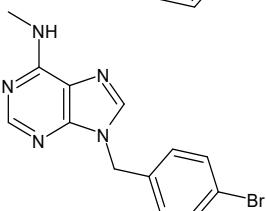
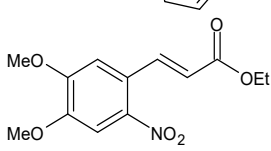
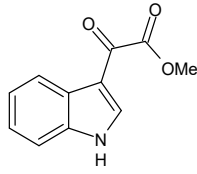
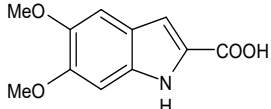
results most similar to the experimentally obtained structure and it was therefore chosen for the docking of all the synthetic compounds.

Docking studies were subsequently carried out on 21 compounds designed in our laboratories and with structural similarity with both rolipram and piclamilast with an exhaustiveness level of 16 for all the molecules under examination (237,238). Some of them are described in the literature for their synthesis and/or biological activities (239-246). Docking studies will help us to verify the possible inhibitory activity of our synthetic molecules and predict the possible interaction on the catalytic site of PDE4 *in vitro*. The different energy levels of molecules under study, along with their molecular structure, are represented in Table 4.

**Table 4.** Energy levels of the first 5 poses out of a total of 9 of each molecule (whose name is indicated in the first column) with an exhaustiveness level of 16, obtained by molecular docking compared to piclamilast and rolipram with the program AutoDock Vina.

compd	structure	1	2	3	4	5
piclamilast		-10.1	-9.5	-9.4	-8.4	-8.4
rolipram		-8.4	-8.4	-8.2	-8.2	-8.1
1		-6.8	-6.8	-6.8	-6.7	-6.6
2		-9.1	-8.6	-8.3	-8.3	-8.0
3		-9.5	-9.4	-9.3	-9.2	-9.0

4		-10.2	-10.0	-9.7	-9.6	-8.6
5		-10.1	-9.9	-9.8	-9.8	-9.6
6		-9.8	-9.5	-9.5	-9.1	-7.9
7		-7.5	-7.5	-7.3	-7.1	-6.9
8		-7.4	-7.1	-7.1	-7.1	-7.0
9		-9.1	-9.1	-8.8	-8.7	-8.6
10		-7.5	-7.3	-7.3	-7.3	-7.1
11		-8.3	-8.3	-8.1	-8.0	-8.0
12		-10.0	-9.1	-8.9	-8.8	-8.6
13		-8.0	-7.6	-7.6	-7.2	-7.1

14		-7.2	-7.0	-6.9	-6.8	-6.2
15		-7.8	-7.7	-7.7	-7.6	-7.3
16		-10.0	-9.9	-9.5	-9.4	-9.3
17		-7.9	-7.9	-7.9	-7.4	-6.8
18		-7.5	-7.2	-7.0	-6.7	-6.5
19		-7.0	-6.9	-6.7	-6.7	-6.6
20		-7.0	-6.5	-6.4	-6.1	-6.1
21		-7.6	-7.3	-7.3	-7.0	-7.0

Both compounds **8** (pose 3) and **17** (pose 1) interact with PDE4B mainly through hydrophobic interactions (Fig. 10A,B). In the docking solutions the two compounds are deeply buried into the active site of PDE4B, which covers about 90% of their accessible



surface area, and are interacting mostly with the same PDE4B residues as well as with the two divalent cations. It is especially noteworthy that aromatic rings of both **8** and **17** form  $\pi$ - $\pi$  interactions with F446, which together with Q443 bind cAMP as part of the active site. Compound **17** makes an additional hydrogen bond with S282 and a very strong bond with  $Mg^{2+}$  (Fig. 10B). Compared to piclamilast and rolipram, which both make two hydrogen bonds with Q443 and otherwise bind many of the same residues and the ions as compound **8** and **17**, these new compounds are interacting with many more residues in the active site, probably due to the potential of their slightly larger size.

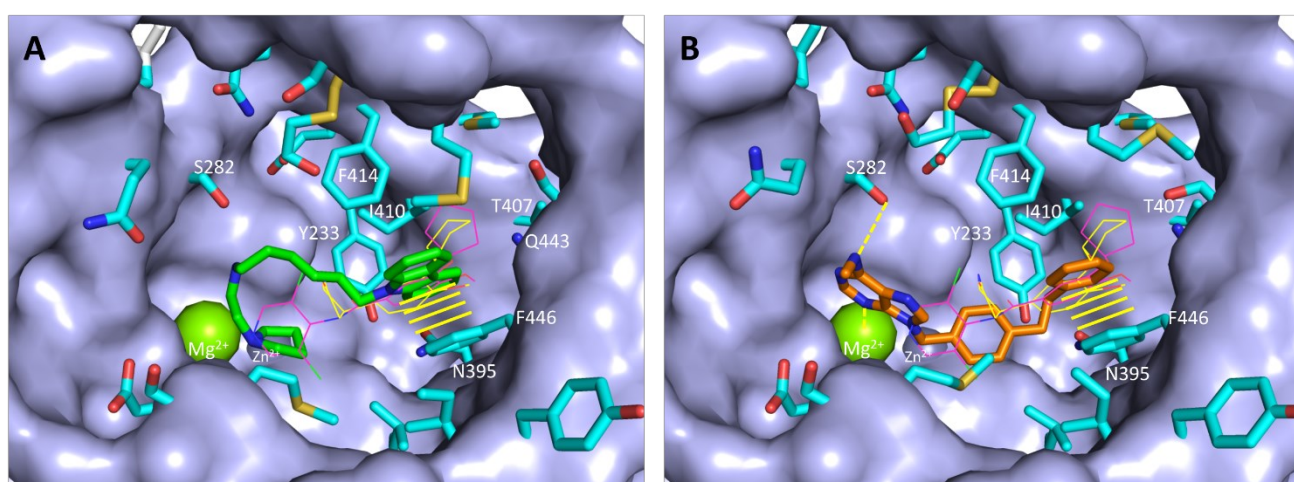


**Figure 10. Docking of compounds 8 and 17 in the active site of PDE4B.** Compound **8** (pose 3 in **A**) is shown with carbons in green and compound **17** (pose 1 in **B**) with carbons in orange. The molecular surface of PDE4B is displayed in light blue and the flexible side chains with carbons in magenta, of which the ones interacting with the ligands are labelled. Strong interactions and hydrogen bonds are indicated with dashed yellow lines and  $\pi$ - $\pi$  interactions with transversal yellow lines. Rolipram and piclamilast are shown in lines with carbons in yellow and magenta, respectively.

### 3.3. Drug Likeness Predictions – Physicochemical - Pharmacokinetic/ADME Properties

Drug-likeness is one of the qualitative ideas employed for predicting drug-like property. It is designated as an intricate balance of diverse molecular and structural features which assesses qualitatively the chance for a molecule to become an oral drug with respect to bioavailability. The targeted molecules were appraised for predicting the Drug-likeness based on 5 separate filters namely Egan, Ghose, Muegge, Veber and Lipinski rules accompanying bioavailability and Drug-likeness scores using the Molsoft software and Swiss ADME program (<http://swissadme.ch>) using the ChemAxon's Marvin JS structure drawing tool (247). Drug-likeness was established from structural or physicochemical inspections of development compounds advanced enough to be considered oral drug-candidates. Drug likeness is examined as an important part that provides the base for the molecules to be a powerful oral drug candidate. Various rules viz. Lipinski, Ghose, Veber, Egan, and Muegge were considered to measure Drug-likeness of the candidate compounds to find out whether they can be bioactive oral drug candidates according to some acute criterion like molecular weight, LogP, number of hydrogen bond acceptors and donors. The number of violations to the above-disclosed rules along with bioavailability and Drug-likeness scores are given in Table 5.

**Table 5.** Drug likeness predictions and Physicochemical-Pharmacokinetic/ADME properties of tested compounds.

No	MW	Number of HBA <sup>a</sup>	Number of HBD <sup>b</sup>	Log $P_{o/w}$ (iLOGP) <sup>c</sup>	Log S <sup>d</sup>	TPSA <sup>e</sup>	BBB permeant <sup>f</sup>	GI absorption	Lipinski, Ghose, Veber, Egan, and Muegge violations	Bioavailability Score	Drug-likeness model score
1	251.24	5	0	2.28	Soluble	81.35	No	High	0	0.55	-1.20
2	318.21	1	0	3.09	Poorly soluble	14.16	Yes	High	0	0.55	-1.11
3	293.41	2	1	3.46	Moderately soluble	20.20	Yes	High	0	0.55	0.40

4	320.45	2	0	0.00	Moderately soluble	11.41	Yes	High	0	0.55	0.09
5	461.38	2	0	0.00	Poorly soluble	11.41	No	High	0	0.55	0.40
6	288.18	0	0	3.02	Poorly soluble	4.93	Yes	High	0	0.55	-1.60
7	328.16	4	1	2.84	Moderately soluble	60.55	Yes	High	0	0.55	-0.46
8	249.26	4	0	3.00	Soluble	49.69	Yes	High	0	0.55	-0.73
9	310.35	3	1	3.04	Moderately soluble	52.49	Yes	High	0	0.55	0.09
10	259.34	2	0	3.07	Moderately soluble	31.23	Yes	High	0	0.55	-0.72
11	309.36	3	0	3.40	Moderately soluble	40.46	Yes	High	0	0.55	-0.77
12	251.32	1	0	2.68	Moderately soluble	20.31	Yes	High	0	0.55	-0.04
13	323.58	3	0	2.51	Moderately soluble	43.60	Yes	High	0	0.55	-0.55
14	323.58	3	0	2.61	Moderately soluble	43.60	Yes	High	0	0.55	-0.38
15	318.17	3	1	2.52	Moderately soluble	55.63	Yes	High	0	0.55	0.07
16	343.42	3	1	3.31	Moderately soluble	55.63	Yes	High	0	0.55	0.37
17	332.20	3	0	2.82	Moderately soluble	48.64	Yes	High	0	0.55	0.12
18	318.17	3	1	2.54	Moderately soluble	55.63	Yes	High	0	0.55	0.10
19	281.26	6	0	2.57	Soluble	90.58	No	High	0	0.55	-1.18
20	203.19	3	1	1.65	Soluble	59.16	Yes	High	0	0.55	-1.30
21	221.21	4	2	1.54	Soluble	71.55	Yes	High	0	0.55	-1.10

a) number of hydrogen bond acceptors; b) number of hydrogen bond donors; c) lipophilicity; d) Water solubility (SILICOS-IT [S=Soluble]); e) topological polar surface area (Å<sup>2</sup>); f) Blood Brain Barrier permeant.

The results revealed that none of the compounds violated any rule and their bioavailability score was around 0.55. All the tested molecules were able to pass the blood-brain barrier (BBB) except compounds **1**, **5** and **19**. All compounds exhibited moderate to good Drug-likeness scores ranged from -1.60 to 0.40. The bioavailability radar of best predicted compounds is displayed in Figure 11. Compounds **8** and **17** appeared to be the

most promising in the *in silico* predictions with a Drug-likeness score of -0.73 and 0.12 respectively, without any rule violation.

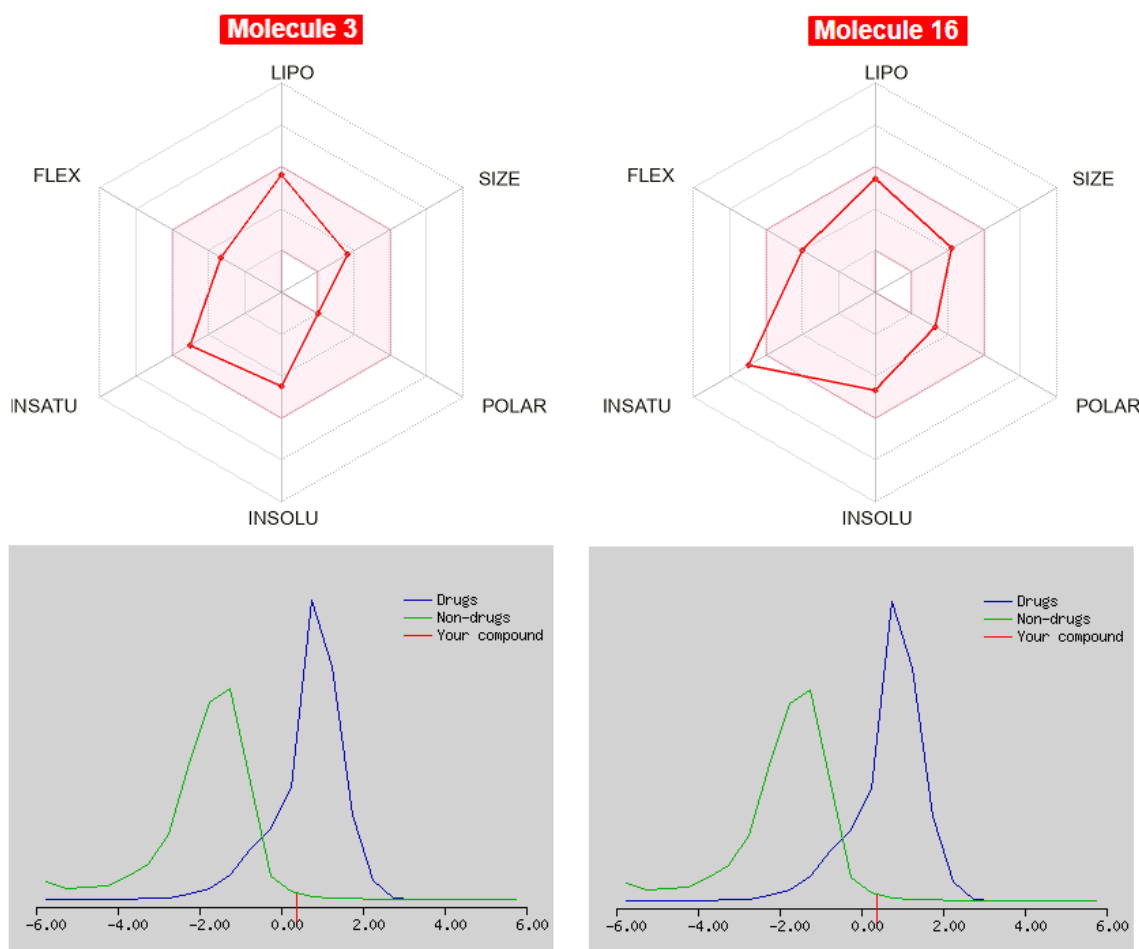


**Figure 11.** Bioavailability Radar of the tested compounds. The pink area represents the optimal range for each property for oral bioavailability, (Lipophilicity (LIPO): XLOGP3 between -0.7 and +5.0, Molecular weight (SIZE): MW between 150 and 500 g/mol, Polarity (POLAR) TPSA between 20 and 130 Å<sup>2</sup>, Solubility (INSOLU): log S not higher than 6, Saturation (INSATU): fraction of carbons in the sp<sup>3</sup> hybridization not less than 0.25, and Flexibility (FLEX): no more than 9 rotatable bonds.

Moreover, all the tested compounds displayed high gastrointestinal (GI) absorption and most of them are P-gp (p-glycoprotein) non-inhibitors. The predictions for the passive BBB permeation, HIA (human gastrointestinal absorption), and P-gp substrates are displayed together in the BOILED-Egg diagram as shown in Figure 12.

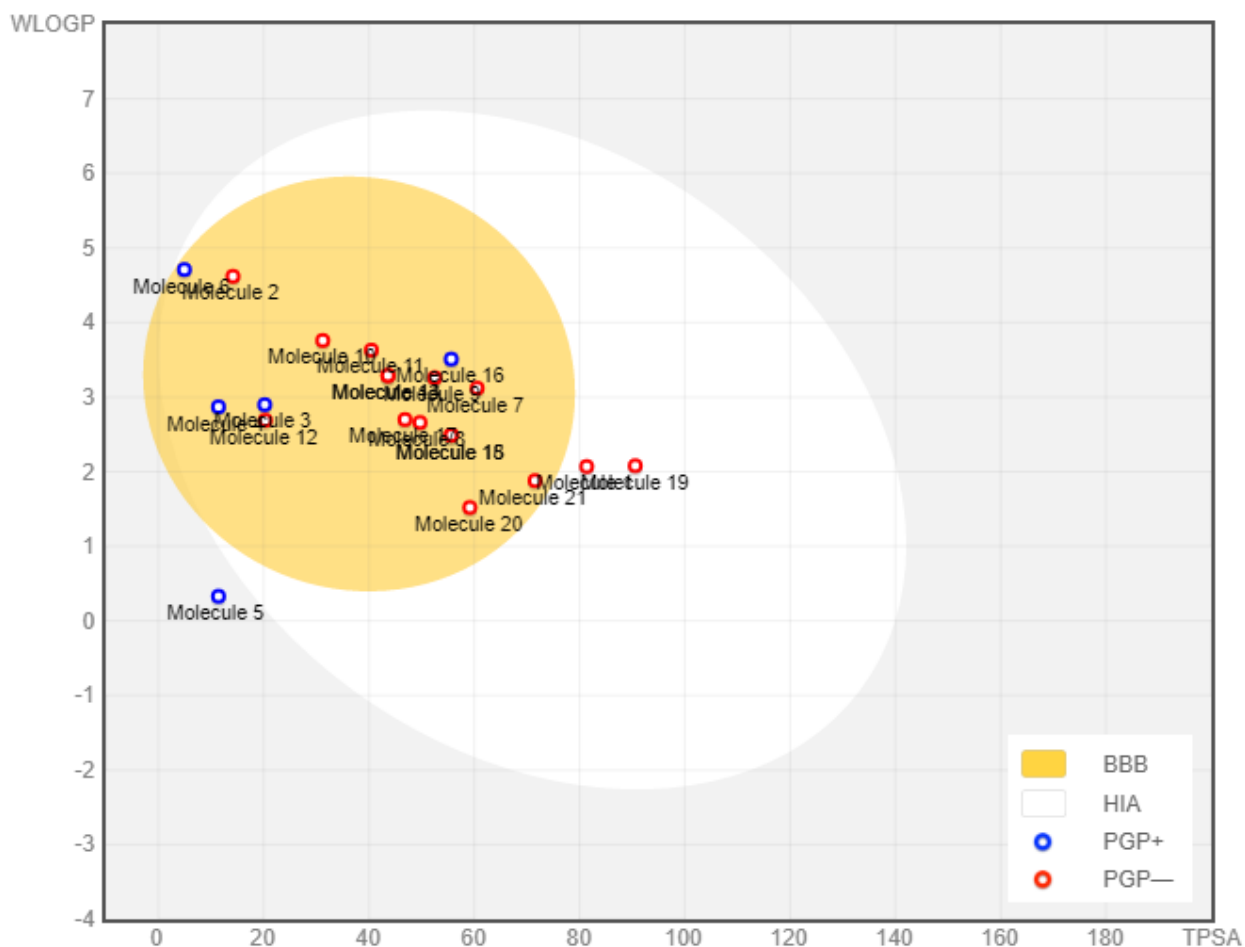


**Figure 12.** BOILED-Egg diagram of the selected compounds 1-21

The early evaluation of ADMET properties of drug candidates play important role in the research and development of new drugs. Taking into account that existing methods for evaluating ADME-Tox properties are expensive and time-consuming and usually require extensive animal testing the computer modeling techniques for ADME-Tox prediction are more preferable method in early drug discovery. Thus, “drug-like” molecules were evaluated in silico for their ADME properties (Table 6) in order to rapidly screen multiple properties (248). Compounds that have been predicted to exhibit high blood-brain barrier, low water solubility and poor Caco2-permeability were excluded from potential hits. The server pkCSM (249) was used for this purpose. pkCSM relies on graph-based signatures. These

encode distance patterns between atoms to represent the small molecule and to train predictive models (250).

**Table 6.** The main pharmacokinetic descriptors studied on pkCSM predictive models.

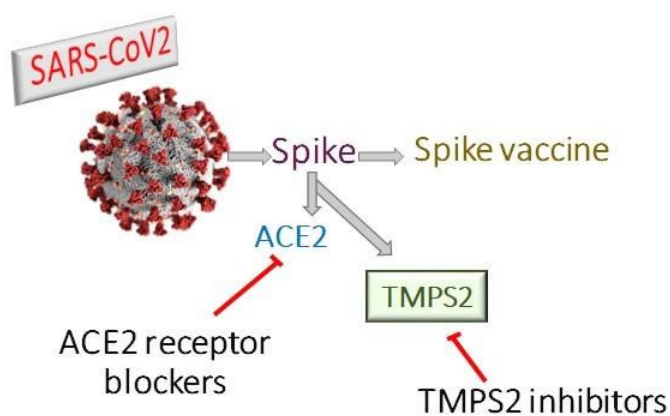
No	Absorption				Distribution		Metabolism	
	Wsol	Caco2	HIA	P-glycoprotein substrate	BBB	CNS	Cyp2d6s	CYP3A4s
1	-3.366	1.002	96.865	No	-0.581	-2.517	No	Yes
2	-6.939	1.072	96.683	Yes	0.895	-1.470	No	Yes
3	-4.182	0.977	92.785	Yes	0.857	-1.937	Yes	Yes
4	-3.913	1.380	94.520	Yes	0.928	-1.617	Yes	Yes
5	-4.419	0.971	92.957	Yes	0.982	-1.561	Yes	Yes
6	-5.837	1.177	96.071	Yes	0.712	-1.321	No	Yes
7	-4.098	1.293	94354	No	0.003	-2.916	No	No
8	-3.293	1.375	97.884	No	-0.011	-2.881	No	No
9	-3.929	1.394	95.590	Yes	0.259	-2.067	No	Yes
10	-3.471	1.368	95.921	No	0.338	-2.159	Yes	Yes
11	-5.694	1.085	95.294	No	0.038	-1.524	No	Yes
12	-3.790	1.730	93.813	No	0.445	-1.020	Yes	Yes
13	-2.650	1.362	92.431	No	-0.345	-1.700	No	Yes
14	-2.688	1.374	92.736	No	0.336	-1.711	No	Yes
15	-2.710	1.315	91.839	No	0.162	-2.738	No	Yes
16	-2.496	0.028	91.873	Yes	0.068	-2.122	No	Yes
17	-2.680	1.326	94.734	No	0.277	-1.743	No	Yes
18	-2.672	1.312	91.268	No	0.166	-2.781	No	Yes
19	-3.844	1.174	97.077	No	-0.815	-2.660	No	Yes
20	-2.012	1.206	94.222	No	-0.169	-2.429	No	No
21	-2.888	1.173	93.615	Yes	-0.320	-3.027	No	No

*WSol*, Water solubility in 25 °C (mg/L); *Caco2*, permeability of *Caco2* cell line (*P<sub>app</sub>* in  $\times 10^{-6}$  cm/s) high permeability of *Caco2* would translate in values > 0.90; *HIA*, human intestinal absorption (% Absorbed); *BBB*, represents the *BBB* permeability as *logBB* (the logarithmic ratio of brain to plasma concentrations) *LogBB*>0.3 cross the brain, while *logBB*<-1 is poorly distributed to the brain; *CNS*, blood-brain permeability-surface area product as (*logPS*) compounds with *logPS*>-2 are considered to penetrate the *CNS*; *CYP2D6s*, substrate for *CYP450* isoform 2D6; *CYP3A4s*, substrate for *CYP450* isoform 3A4.

In order to identify new molecules to be investigated for the fight against COVID-19, a docking study, through the AutoDock Vina program, was carried out. The possible interactions of twenty-one in house compounds with the catalytic site of the A chain of PDE4B were investigated, identifying the poses of the molecules with high similarity to piclamilast and rolipram in the most favorable spatial conformation of interaction with the catalytic site of PDE4B. These compounds were inserted into the pocket of the catalytic site of the PDE4B and in many cases they overlapped piclamilast almost completely. The obtained results indicated that the designed compounds may represent promising ligands for PDE4B receptors and therefore they deserve further in-depth *in vitro* studies. Moreover, Drug-likeness were carried out on these compounds. The most interesting compounds in the *in silico* predictions were **8** and **17** showing Drug-likeness scores of -0.73 and 0.12, respectively, without any rule violation.

### 3.4 Design of Human Transmembrane Protease Serine-2 (TMPS2) Inhibitors Guanidine Derivatives against SARS-CoV-2 Infection

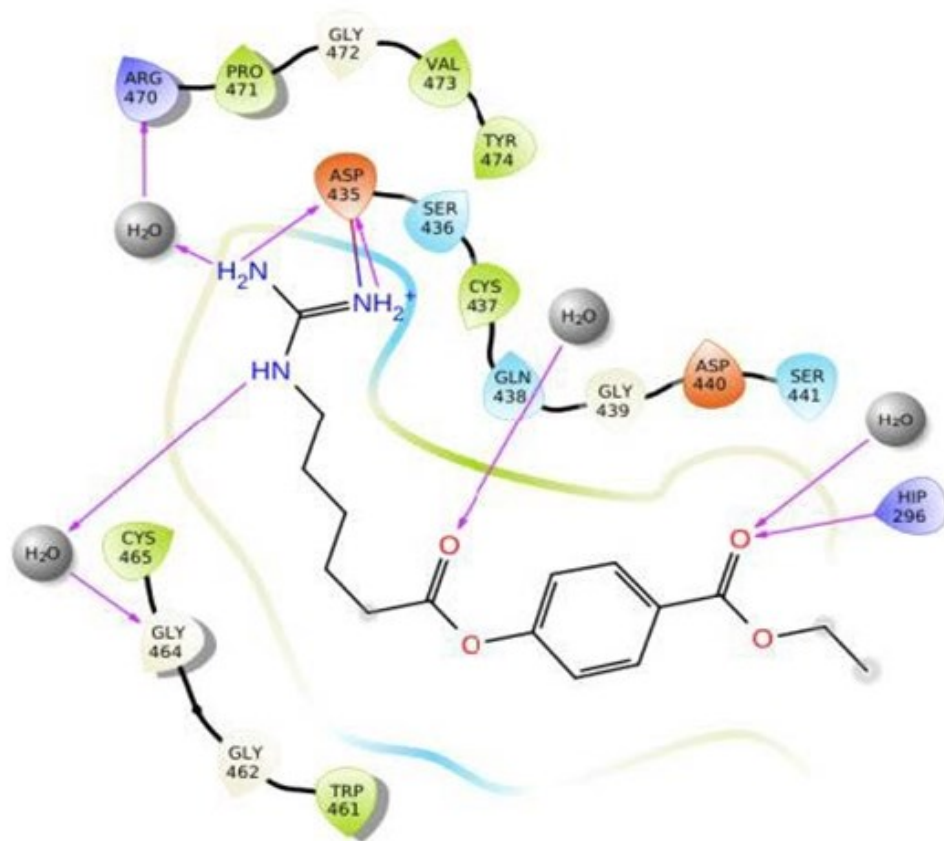
The SARS-CoV-2 infection depends on the host cell ACE2 and TMPS2, where the virus uses ACE2 for entry and TMPS2 for S protein priming. The TMPS2 gene encodes a Transmembrane Protease Serine-2 protein (TMPS2) that belongs to the serine protease family (Figure 13) (251). Docking of TMPS2 inhibitors (camostat, nafamostat, gabexate), using Auto dock Vina software, into the constructed model was performed and the protein-ligand complexes were subjected to MD simulations and computational binding affinity calculations. After these studies, we designed some guanidine derivatives, which were then synthesized. These studies determined the tertiary structure of TMPS2 amino acid sequence and predicted how our synthetic guanidine derivatives bind to the model, which is important for drug development for the prevention and treatment of COVID-19. We subsequently carried out molecular docking studies with our guanidine-structured molecules to select those that bind more in relation to the bond between gabesate and TMPS2. Below, structures of the gabesate and our synthetic compounds, are reported, in pymol format, necessary to carry out the molecular docking through the Auto dock Vina program. The synthesis of the selected molecules is in progress; *in vitro* studies on the virus and cytotoxicity studies on non-infected human cells will then be performed.



**Figure 13.** Therapeutic approaches for treatment of COVID-19 either by ACE2 receptor blockers, TMPS2 inhibitors or spike vaccine.



The research project involves the design of molecules that prevent the binding with the ACE2 receptor, together with the design and synthesis of molecules capable of reducing oxidation and inflammation processes. At the same time, a molecular docking study had to be carried out on several classes of molecules and on selected targets involved (spike protein, ACE2 receptor, TMPRSS2 serineprotease). Docking of TMPRSS2 inhibitors, camostat, nafamostat, gabexate, using Auto dock Vina software, into the constructed model was performed and the protein-ligand complexes were subjected to MD simulations and computational binding affinity calculations. After these studies, new guanidine derivatives were designed and synthesized. These studies determined the tertiary structure of TMPRSS2 amino acid sequence and predicted how our synthetic guanidine derivatives bind to the model, which is an important goal in drug development for the prevention and treatment of COVID-19. We subsequently carried out molecular docking studies with our guanidine-structured molecules to select those that bind more in relation to the bond between gabexate and TMPRSS2 (Fig. 14) (252,253).

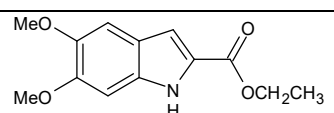
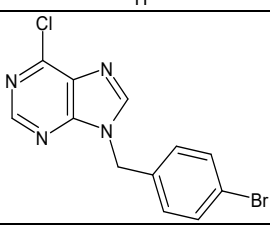
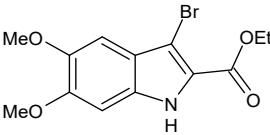
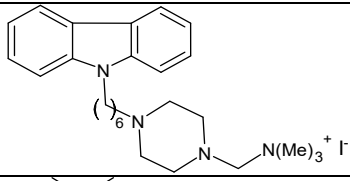
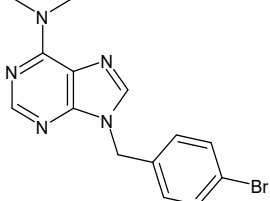


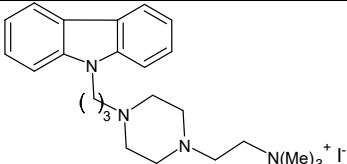
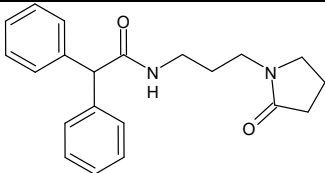
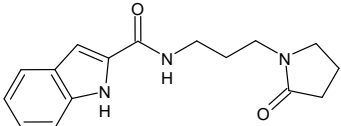
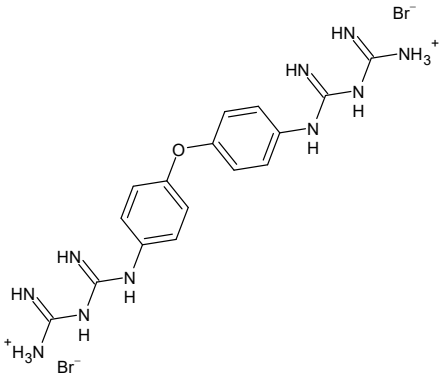
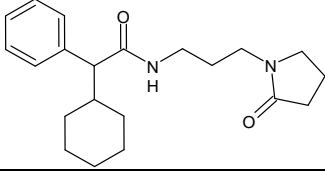
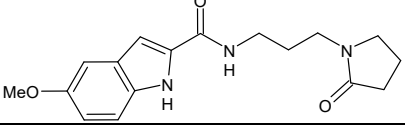
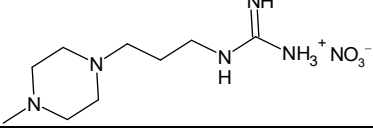
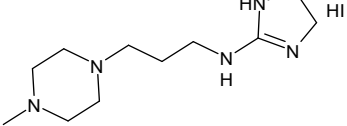
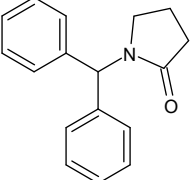
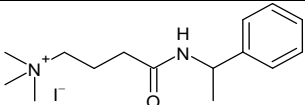
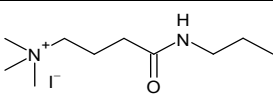
*Figure 14. Interaction between gabesate and domain of the TMPS2*

## CHAPTER 4 – Results and Discussion

The compounds that had given the most interesting results in molecular docking studies for the inhibition of PDE4B were synthesized along with the compounds structurally related to gabesate that possessed the chemical characteristics capable of interacting with the pocket binding to the ACE2 receptor. For the PDE4B the most interesting compounds that gave encouraging results in molecular docking studies were compounds **M1** and **M5** (**8** and **17** in ref. 254, respectively). Then, *in vitro* tests were carried out on these samples. The studied compounds are summarized in Table 7. The purity of the new compounds was assessed by elemental analysis.

**Table 7.** Structures of the studied compounds

Structure	Compd	Number in ref. (254)	Elemental analysis
	<b>M1</b>	<b>8</b>	Ref. 254
	<b>M2</b>	<b>14</b>	Ref. 254
	<b>M3</b>	<b>7</b>	Ref. 254
	<b>M4</b>	<b>5</b>	Ref. 254
	<b>M5</b>	<b>17</b>	Ref. 254

	<b>M8</b>	<b>4</b>	Ref. 254
	<b>FG1</b>	-	C <sub>21</sub> H <sub>24</sub> N <sub>2</sub> O <sub>2</sub> FW = 336,44
	<b>FG2</b>	-	C <sub>16</sub> H <sub>19</sub> N <sub>3</sub> O <sub>2</sub> FW = 285,35
	<b>FG3</b>	-	C <sub>16</sub> H <sub>22</sub> Br <sub>2</sub> N <sub>10</sub> O FW = 530,23
	<b>FG4</b>	-	C <sub>21</sub> H <sub>30</sub> N <sub>2</sub> O <sub>2</sub> FW = 342,48
	<b>FG5</b>	-	C <sub>17</sub> H <sub>21</sub> N <sub>3</sub> O <sub>3</sub> FW = 315,37
	<b>FG6</b>	-	C <sub>9</sub> H <sub>22</sub> N <sub>6</sub> O <sub>3</sub> FW = 262,31
	<b>FG7</b>	-	C <sub>11</sub> H <sub>24</sub> IN <sub>5</sub> FW = 353,25
	<b>FG8</b>	<b>12</b>	C <sub>17</sub> H <sub>17</sub> NO FW = 251,33
	<b>FG9</b>	-	C <sub>15</sub> H <sub>25</sub> IN <sub>2</sub> O FW = 376,28
	<b>FG10</b>	-	C <sub>10</sub> H <sub>23</sub> IN <sub>2</sub> O FW = 314,21

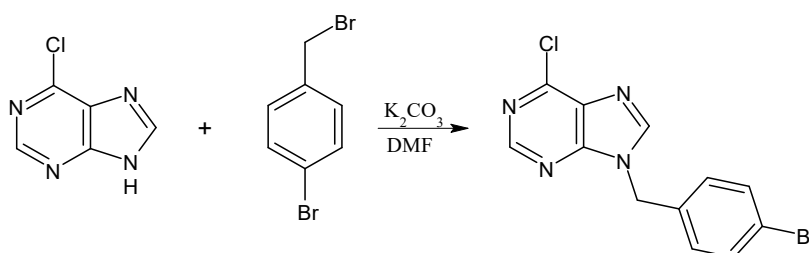
Specifically, PDE4B inhibition studies were carried out on compounds **M1–M8**.

ACE2 receptor inhibition was studied for three classes of compounds:

- 1) Class A – pyrrolidinone derivatives: **FG1, FG2, FG4, FG5** and **FG8**
- 2) Class B – guanidine or biguanidine derivatives: **FG3, FG6** and **FG7**
- 3) Class C – quaternary salts: **FG9** and **FG10**

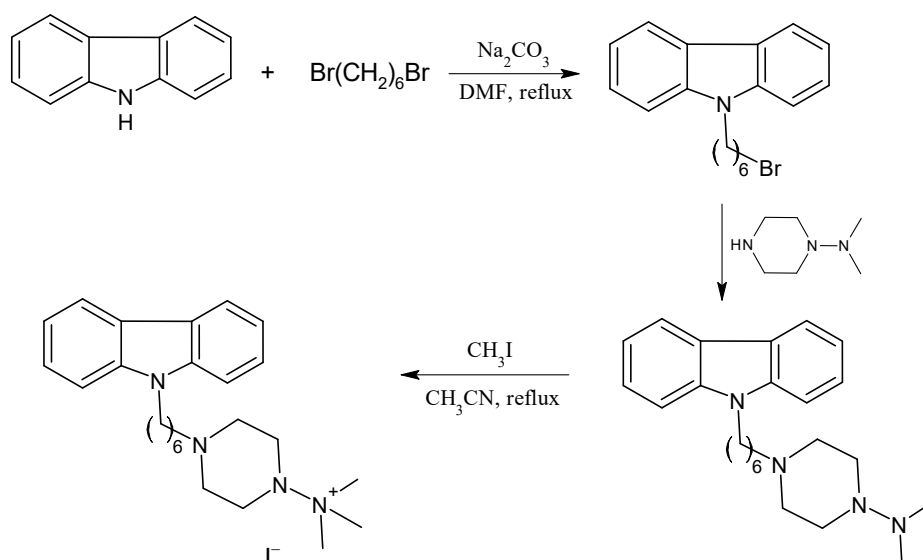
## 4.1. Chemistry

The synthesis of compound **M2** (9-[(4-bromophenyl)methyl]-6-chloro-9*H*-purine) is shown in Scheme 1. 6-Chloropurine was reacted with 4-bromobenzyl bromide in the presence of potassium carbonate in *N,N*-dimethylformamide.



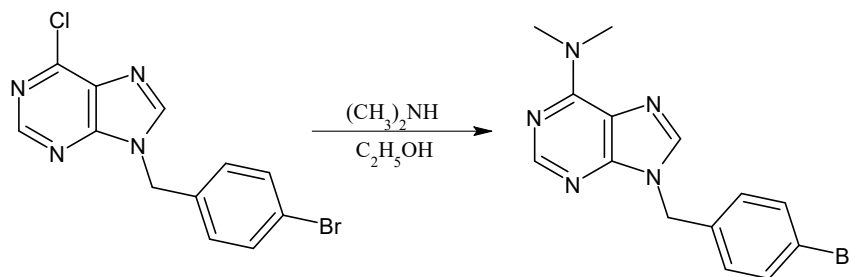
**Scheme 1.** Synthesis of compound **M2** (Sample 14)

Compound **M4** (4-[(9*H*-carbazol-9-yl)methyl]-*N,N*-dimethylpiperazin-1-amine) was prepared as depicted in Scheme 2. Carbazole was reacted with 1,6-dibromohexane in the presence of sodium carbonate in DMF under reflux. The bromo derivative obtained was reacted with *N,N*-dimethylpiperazin-1-amine. The amine was then converted into its iodide salt by reaction with iodomethane in acetonitrile under reflux.



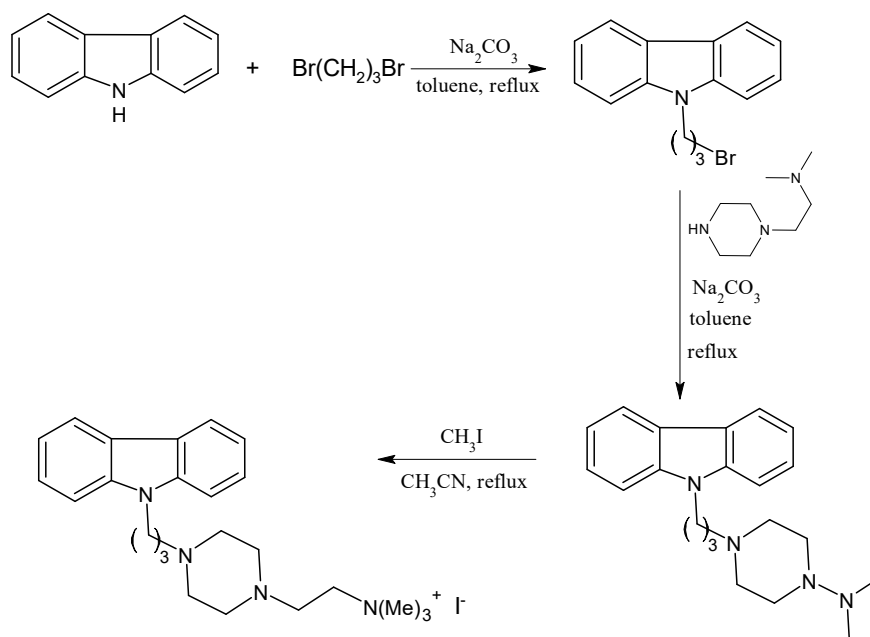
**Scheme 2.** Synthesis of compound **M4**

Compound **M5** (9-[(4-bromophenyl)methyl]-*N,N*-dimethyl-9*H*-purin-6-amine) was obtained as reported in Scheme 3. 9-[(4-Bromophenyl)methyl]-6-chloro-9*H*-purine, prepared as above described, was reacted with dimethylamine in ethanol to give the desired compound.



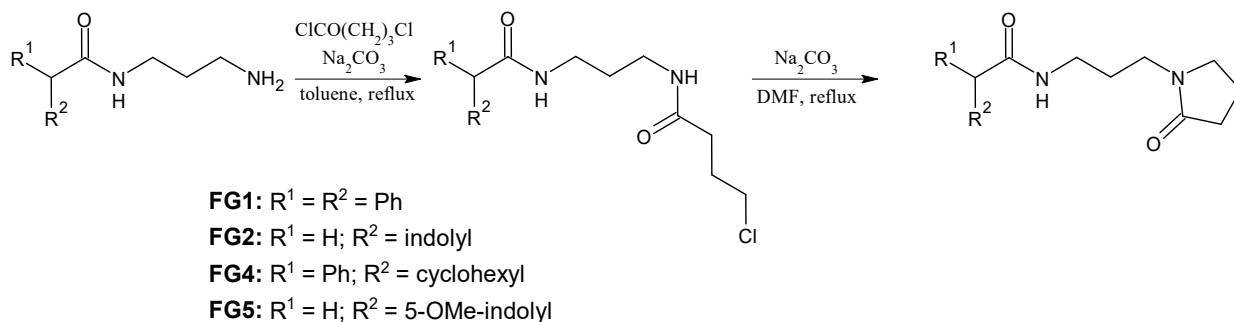
**Scheme 3.** Synthesis of compound **M5**

Compound **M8** (4-[(9*H*-carbazol-9-yl)methyl]-*N,N*-dimethylpiperazin-1-amine) was prepared as depicted in Scheme 4. Carbazole was reacted with 1,3-dibromopropane in the presence of sodium carbonate in toluene under reflux. The bromide obtained was then reacted with *N,N*-dimethyl-2-(4-methylpiperidin-1-yl)ethanamine in the presence of sodium carbonate in toluene under reflux. The amine was then converted into its iodide salt by reaction with iodomethane in acetonitrile under reflux.



**Scheme 4.** Synthesis of compound **M8**

Pyrrolidinone derivatives belonging to class A (**FG1**, **FG2**, **FG4**, **FG5** and **FG8**) were synthesized as described below. Specifically, the synthetic route to compounds **FG1**, **FG2**, **FG4** and **FG5** is depicted in Scheme 5. *N*-(3-aminopropyl)aklylamides were reacted with 4-chlorobutyryl chloride in the presence of Na<sub>2</sub>CO<sub>3</sub> in toluene under reflux. The amido derivative obtained was cyclized to the corresponding pyrrolidinone derivative.



**Scheme 5.** Synthesis of compounds **FG1**, **FG2**, **FG4** and **FG5**



## 4.2. *In Vitro* Studies

### 4.2.1. *Studies on Human PDE4B*

The effect of synthesized compounds was evaluated by using the Human PDE4B (cAMP-specific 3',5'-cyclic phosphodiesterase 4B) ELISA Kit, a quantitative sandwich enzyme immunoassay. The results of ELISA immunoassay are shown in Figure 15. The intensity of colored product significantly decreased in the presence of 100 nM of both compounds **M1** and **M2**. When the compounds were used at the concentration of 10  $\mu$ M, a reduction was obtained after treatment with **M1**, **M2**, **M3** and **M6**. These preliminary results indicated that **M1**, **M2**, **M3** and **M6** bind to human PDE4B by impacting on the interaction with the specific antibody and potentially by affecting PDE4B activity.

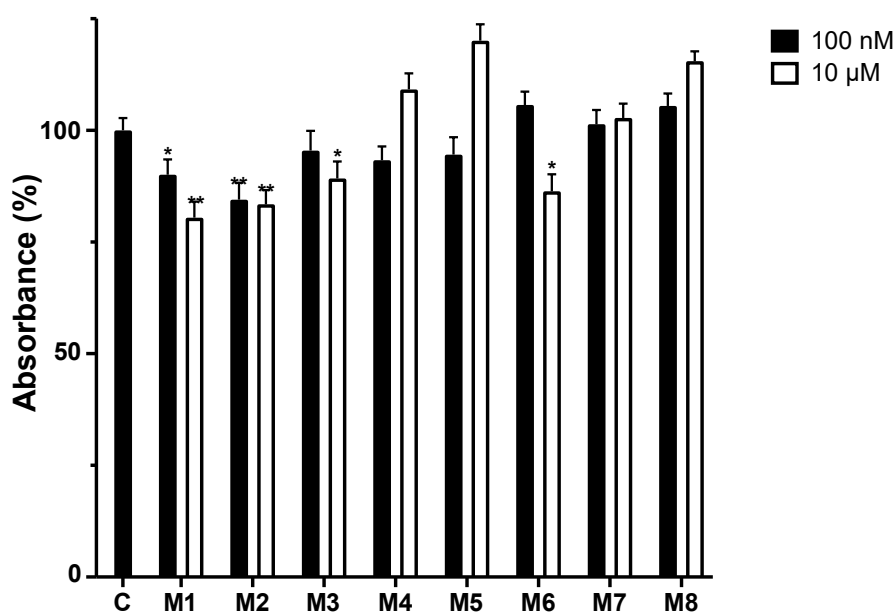


**Figure 15.** Results of ELISA immunoassay for human PDE4B are reported. These preliminary results indicated that **M1**, **M2**, **M3** and **M6** bind to human PDE4B by impacting the interaction with the specific antibody and potentially by affecting PDE4B activity.

#### 4.2.2. Angiotensin II Converting Enzyme (ACE2) Inhibition Studies

Compounds **FG1–FG10** were studied for their inhibiting activity of ACE2. The stock solutions of all the molecules (FG1:FG10) were prepared by solubilizing the powders in DMSO, thus obtaining a starting concentration of 10 mM for all. ACE2 activity was measured using Angiotensin II Converting Enzyme (ACE2) Inhibitor Screening Kit (cat. No. MAK378, Sigma-Aldrich, St. Louis, MO, USA). The assay was performed in triplicate, using an aliquot of 10  $\mu$ L of each sample and following the manufacturer's protocol. The inhibitory activity of all ten molecules was evaluated at a final concentration of both 10  $\mu$ M and 1  $\mu$ M. Fluorescence was read using a VICTOR Nivo Multimode Microplate Reader (PerkinElmer). The % relative inhibition of each molecule determined at the concentration 10  $\mu$ M and 1  $\mu$ M are reported in the tables below. The compounds with the greatest inhibitory action on the ACE2 receptor are **FG1** and **FG2**.

<b>SAMPLE (10 <math>\mu</math>M)</b>	<b>% Inhibition</b>
ACE2	0
ACE2 + Commercial Inhibitor	98,66526569
ACE2 + FG1	-6,632252664
ACE2 + <b>FG2</b>	<b>5,646919307</b>
ACE2 + FG3	-10,51254774
ACE2 + FG4	-10,03121676
ACE2 + FG5	-4,305819571
ACE2 + <b>FG6</b>	<b>5,939903385</b>
ACE2 + FG7	2,275858461
ACE2 + FG8	-7,865227324
ACE2 + FG9	0,408084965
ACE2 + <b>FG10</b>	<b>8,381437366</b>

<b>SAMPLE (1 <math>\mu</math>M)</b>	<b>% Inhibition</b>
ACE2	0
ACE2 + Commercial Inhibitor	-20,40599222
ACE2 + <b>FG1</b>	<b>20,62224237</b>
ACE2 + <b>FG2</b>	<b>25,14082419</b>
ACE2 + <b>FG3</b>	<b>6,80141609</b>
ACE2 + FG4	-25,80003837
ACE2 + FG5	1,072530999
ACE2 + FG6	-6,688059155
ACE2 + FG7	0,709788807
ACE2 + FG8	-7,696063898
ACE2 + FG9	0,340070804
ACE2 + FG10	-20,40599222

## **CHAPTER 5 – Materials and Methods**

### **5.1. Chemistry**

The progress of the reactions and the purity of the synthesized products were monitored by thin layer chromatography (TLC), using aluminum plates covered with Whatman K6F silica gel (or Merck-25 DC-Alufolien Kiesegel 60 F254) and alumina (Merck) with fluorescence indicators, using the appropriate eluents and observed under ultraviolet light (254 nm). The organic extracts were dried on anhydrous sodium sulphate (Merck) or on anhydrous magnesium sulphate (Riedel - De Haen). The melting points were determined with Gallenkam apparatus. As solid supports for liquid chromatography adsorption were employed Silica Gel 60 (Merck) and Alumina 90 (Merck) and celite 545. The concentration of the solutions, after reaction and extraction, was carried out at reduced pressure with a Buchi Rotavapor apparatus. IR spectra were performed in KBr with a Shimatsu 8000 spectrophotometer. <sup>1</sup>H NMR spectra were obtained with Bruker Advance 300 and 600 spectrometers MHz using DMSO-*d*<sub>6</sub> as solvent, at the Faculty of Pharmacy of L. University. Pasteur I of Strasbourg and at the Faculty of Pharmacy of the University of Salerno. The mass spectra were carried out with a Finnigan LCQ Deca spectrophotometer, at the Mass Spectrometry center of the CNR in Cosenza.

### **5.2. Human PDE4B Elisa Assay**

The Human PDE4B (cAMP-specific 3',5'-cyclic phosphodiesterase 4B) ELISA Kit (Code number: HUEB0664 Creative Diagnostics, Shirley, NY), a quantitative sandwich enzyme immunoassay, was carried out following the manufacturer's recommendations. Briefly, the human PDE4B (5 ng/mL) was incubated in a 96-well plate together with a biotinylated antibody specific for PDE4B, in the presence of absence of synthesized

molecules (**M1–M8**) at the concentration of 100 nM and 10  $\mu$ M, respectively. Each compound was dissolved in DMSO to make stock solutions and then sterile water was used for dilutions. After incubation and washing, the enzyme Streptavidin- horseradish peroxidase (Streptavidin-HRP) was added, incubated and washed. The binding between the enzyme Streptavidin-HRP and the biotinylated antibody specific for PDE4B, carried out in the presence of 3,3',5,5'-tetramethylbenzidine (TMB) substrate, induced the formation of the colored reaction product. In our experiments, we related the intensity of coloration to the interaction between human PDE4B and synthetic molecules which can inhibit the antibody's ability to bind.

### **5.3. Angiotensin II Converting Enzyme (ACE2) Inhibition Screening Studies**

The stock solutions of all the molecules (**FG1–FG10**) were prepared by solubilizing the powders in DMSO, thus obtaining a starting concentration of 10 mM for all. ACE2 activity was measured using Angiotensin II Converting Enzyme (ACE2) Inhibitor Screening Kit (cat. No. MAK378, Sigma-Aldrich, St. Louis, MO, USA). The assay was performed in triplicate, using an aliquot of 10  $\mu$ L of each sample and following the manufacturer's protocol. The inhibitory activity of all ten molecules was evaluated at a final concentration of both 10  $\mu$ M and 1  $\mu$ M. Fluorescence was read using a VICTOR Nivo Multimode Microplate Reader (PerkinElmer). Two time points were chosen (T1=105s and T2=370s, in the linear range of the graph) and the corresponding fluorescence values were obtained (RFU1 and RFU2, RFU = Relative Fluorescence Unit). The slopes were therefore calculated for all the samples, and it was possible to calculate the % relative inhibition of each molecule using the formula:

$$\% \text{ Relative Inhibition} = \frac{\text{Slope EC} - \text{Slope S}}{\text{Slope EC}} * 100$$

(EC = Enzyme control (ACE2, no inhibition), S = sample (ACE2 + molecule))

## CHAPTER 6 – CONCLUSIONS

The novel COVID-19 continues to endanger human health, and the therapeutic drugs for its treatment are under intensive research and development. Identifying the efficacy and toxicity of drugs in animal models is helpful for further screening of effective medications, which is also a prerequisite for drugs to enter clinical trials. SARS-CoV-2 invades host cells mainly by the S protein on its surface. After the SARS-CoV-2 RNA genome is injected into the cells, Mpro will help assemble and release new viruses. RdRp is crucial for virus replication, assembly, and release of new virus particles. Among the new strategies for the treatment of COVID-19, many scientific and effective methods have been studied, such as computer drug design technology or structure detection by using macromolecular docking analysis to target the interaction and affinity between drugs and SARS-CoV-2. In addition, drug similarity characteristics can also be evaluated to determine whether it has the potential to become a standard for drugs. If the standard is established, it can further detect the ADMET of potential candidate drugs by using human or humanized tissue functional proteins as “drug targets”. *In vitro* research techniques combine with computer simulation methods may lead to the discover of a new “lead compound”. Studying the ADMET, that is the interaction between drugs and biophysical, biochemical barrier factors in the body, not only determines the safety of the drugs, but also provides reference for pharmacokinetic characteristics. The study of drug efficacy and toxicity in experimental animals and animal models is an important guarantee to promote the development of new drugs, which is helpful to explore the bioavailability of drugs or to develop new therapies together with other drugs. The results obtained *in vitro* with our compounds, structurally designed and synthesized on the basis of molecular docking studies, allowed us to identify potential inhibitors of both PDE4B and ACE2 receptors. In the future, these molecules will be subjected to *in vivo* tests, in order to evaluate their real effectiveness and possible toxicity. Many of these molecules,

in addition to having a possible usefulness in SARS-Cov-2 infection, may have important possible uses in other diseases such as pulmonary hypertension, asthma and arterial hypertension. Thanks to this work, we therefore lay the foundations for a future *in vivo* study that could bring new therapies to the medical field as well as to SARS-CoV-2 infection.

## References

1. Chen, Y.; Chen, L.; Deng, Q.; Zhang, G.; Wu, K.; Ni, L.; et al. “The Presence of SARS-CoV-2 RNA in the Feces of COVID-19 Patients.” **J. Med. Virol.** 2020, 92 (4), 418–442.
2. Chan, J.F.W.; Kok, K.H.; Zhu, Z.; Chu, H.; To, K.K.W.; Yuan, S.; Yuen, K.Y. “Genomic Characterization of the 2019 Novel Human-Pathogenic Coronavirus Isolated from a Patient with Atypical Pneumonia after Visiting Wuhan.” **Emerg. Microb. Infect.** 2020, 9 (1), 221–223.
3. Hoffmann, M.; Kleine-Weber, H.; Schroeder, S.; Krüger, N.; Herrler, T.; Erichsen, S.; et al. “SARS-CoV 2 Cell Entry Depends on ACE2 and TMPRSS2 and Is Blocked by a Clinically Proven Protease Inhibitor.” **Cell** 2020, 181, 271–280.
4. Tao, Z.; Tian, J.; Pei, Y.; Yuan, M.; Zhang, Y.; Dai, F. “A New Coronavirus Associated with Human Respiratory Disease in China.” **Nature** 2020, 579, 265–269.
5. Barile, E.; Baggio, C.; Gambini, L.; Shiryayev, S.A.; Strongin, A.Y.; Pellicchia, M. “Potential Therapeutic Targeting of Coronavirus Spike Glycoprotein Priming.” **Molecules** 2020, 25, 2424.

6. Shirato, K.; Kawase, M.; Matsuyama, S. “Wild-type Human Coronaviruses Prefer Cell-surface TMPRSS2 to Endosomal Cathepsins for Cell Entry.” **J. Virol.** 2020, 517, 9–15.
7. Eleftheriou, P.; Amanatidou, D.; Petrou, A.; Geronikaki, A. “In Silico Evaluation of the Effectivity of Approved Protease Inhibitors against the Main Protease of the Novel SARS-CoV-2 Virus.” **Molecules** 2020, 25, 2529.
8. Dong, M.; Zhang, J.; Ma, X. “ACE2, TMPRSS2 Distribution and Extrapulmonary Organ Injury in Patients with COVID-19.” **Biomed. Pharmacother.** 2020, 131, 110678.
9. Guarner, J. “Three Emerging Coronaviruses in Two Decades: The Story of SARS, MERS, and Now COVID-19.” **Am. J. Clin. Pathol.** 2020, 153, 420–421.
10. Lu, R.; Zhao, X.; Li, J.; Niu, P.; Yang, B.; Wu, H. “Genomic Characterisation and Epidemiology of 2019 Novel Coronavirus: Implications for Virus Origins and Receptor Binding.” **Lancet** 2020, 395, 565–574.
11. Gorbalenya, A.E.; Baker, S.C.; Baric, R.S.; de Groot, R.J.; Drosten, C.; Gulyaeva, A.A.; et al. “Severe Acute Respiratory Syndrome-related Coronavirus: Classifying 2019-nCoV and Naming it SARS-CoV-2.” **Nat. Microbiol.** 2020, 5(4,5), 536–544.
12. WHO Director-General’s remarks at the media briefing on 2019-nCoV on 11 February 2020. <https://www.who.int/director-general/speeches/detail/who-director-general-s-remarks-at-the-media-briefing-on-2019-ncov-on-11-february-2020> (Accessed on 25 October 2023).
13. Andersen, K.G.; Rambaut, A.; Lipkin, W.I.; Holmes, E.C.; Garry, R.F. “The proximal Origin of SARS-CoV-2.” **Nat. Med.** 2020, 26(4), 450–452.
14. Temmam, S.; Vongphayloth, K.; Baquero, E.; Munier, S.; Bonomi, M.; Regnault, B.; et al. “Bat Coronaviruses Related to SARS-CoV-2 and Infectious for Human Cells.” **Nature** 2022, 604, 330–336.
15. Zhou, F.; Yu, T.; Du, R.; Fan, G.; Liu, Y.; Liu, Z.; et al. “Clinical Course and Risk Factors for Mortality of Adult Inpatients with COVID-19 in Wuhan, China: A Retrospective Cohort Study.” **Lancet** 2020, 395, 1054–1062.
16. Guan, W.J.; Ni, Z.Y.; Hu, Y.; Liang, W.H.; Ou, C.Q.; He, J.X.; et al. “Clinical Characteristics of Coronavirus Disease 2019 in China.” **N. Engl. J. Med.** 2020, 382, 1708–1720.
17. Huang, C.; Wang, Y.; Li, X.; Ren, L.; Zhao, J.; Hu, Y.; et al. “Clinical Features of Patients Infected with 2019 Novel Coronavirus in Wuhan, China.” **Lancet** 2020, 395, 497–506.



18. Lauer, S.A.; Grantz, K.H.; Bi, Q.; Jones, F.K.; Zheng, Q.; Meredith, H.R., et al. “The Incubation Period of Coronavirus Disease 2019 (CoVID-19) from Publicly Reported Confirmed Cases: Estimation and Application.” **Ann. Intern. Med.** 2020, 172, 577–582.
19. Bai, Y.; Yao, L.; Wei, T.; Tian, F.; Jin, D.Y.; Chen, L.; Wang, M. “Presumed Asymptomatic Carrier Transmission of COVID-19.” **JAMA** 2020, 323, 1406–1407.
20. He, X.; Lau, E.H.; Wu, P.; Deng, X.; Wang, J.; Hao, X.; et al. “Temporal Dynamics in Viral Shedding and Transmissibility of COVID-19.” **Nat. Med.** 2020, 26, 672–675.
21. Rothan, H.A.; Byrareddy, S.N. “The Epidemiology and Pathogenesis of Coronavirus Disease (COVID-19) Outbreak.” **J. Autoimmun.** 2020, 109, 102433.
22. Wiersinga, W.J.; Rhodes, A.; Cheng, A.C.; Peacock, S.J.; Prescott, H.C. “Pathophysiology, Transmission, Diagnosis, and Treatment of Coronavirus Disease 2019 (COVID-19): A Review.” **JAMA** 2020, 324, 782–793.
23. Petersen, E.; Koopmans, M.; Go, U.; Hamer, D.H.; Petrosillo, N.; Castelli, F.; et al. “Comparing SARS-CoV-2 with SARS-CoV and Influenza Pandemics.” **Lancet Infect. Dis.** 2020, 20, e238–e244.
24. COVID Live - Coronavirus Statistics - Worldometer. <https://www.worldometers.info/coronavirus/> (Accessed on 23 October 2023).
25. Chu, D.K.; Akl, E.A.; Duda, S.; Solo, K.; Yaacoub, S.; Schünemann, H.J.; et al. “Physical Distancing, Face Masks, and Eye Protection to Prevent Person-to-person Transmission of SARS-CoV-2 and COVID-19: A Systematic Review and Meta-analysis.” **Lancet** 2020, 395, 1973–1987.
26. Wilder-Smith, A.; Freedman, D.O. “Isolation, Quarantine, Social Distancing and Community Containment: Pivotal Role for Old-style Public Health Measures in the Novel Coronavirus (2019-nCoV) Outbreak.” **J. Travel. Med.** 2020, 27, taaa020. Doi: 10.1093/jtm/taaa020.
27. Remuzzi, A.; Remuzzi, G. “COVID-19 and Italy: What Next?” **Lancet** 2020, 395, 1225–1228.
28. Ranney, M.L.; Griffeth, V.; Jha, A.K. “Critical Supply Shortages — The Need for Ventilators and Personal Protective Equipment during the Covid-19 Pandemic.” **N. Engl. J. Med.** 2020, 382, e41.
29. Grasselli, G.; Pesenti, A.; Cecconi, M. “Critical Care Utilization for the COVID-19 Outbreak in Lombardy, Italy: Early Experience and Forecast During an Emergency Response.” **JAMA** 2020, 323, 1545–1546.

30. Pan, A.; Liu, L.; Wang, C.; Guo, H.; Hao, X.; Wang, Q.; et al. "Association of Public Health Interventions With the Epidemiology of the COVID-19 Outbreak in Wuhan, China." **JAMA** 323, 1915–1923 (2020).
31. Giordano, G.; Blanchini, F.; Bruno, R.; Colaneri, P.; Di Filippo, A.; Di Matteo, A.; Colaneri, M. "Modelling the COVID-19 Epidemic and Implementation of Population-Wide Interventions in Italy." **Nat. Med.** 2020 26(6), 855–860.
32. Nicola, M.; Alsafi, Z.; Sohrabi, C.; Kerwan, A.; Al-Jabir, A.; Iosifidis, C.; et al. "The Socio-Economic Implications of the Coronavirus Pandemic (COVID-19): A Review." **Int. J. Surg.** 2020, 78, 185–193.
33. Rajkumar, R.P. "COVID-19 and Mental Health: A Review of the Existing Literature." **Asian J. Psychiatr.** 2020, 52, 102066.
34. Emanuel, E.J.; Persad, G.; Upshur, R.; Thome, B.; Parker, M.; Glickman, A.; et al. "Fair Allocation of Scarce Medical Resources in the Time of Covid-19." **N. Engl. J. Med.** 2020, 382, 2049–2055.
35. Schlander, M.; Hernandez-Villafuerte, K.; Cheng, C.Y.; Mestre-Ferrandiz, J.; Baumann, M. "How Much Does It Cost to Research and Develop a New Drug? A Systematic Review and Assessment." **Pharmacoeconomics** 2021, 39, 1243–1269.
36. Liu, C.; Zhou, Q.; Li, Y.; Garner, L.V.; Watkins, S.P.; Carter, L.J.; et al. "Research and Development on Therapeutic Agents and Vaccines for COVID-19 and Related Human Coronavirus Diseases." **ACS Cent. Sci.** 2020, 6, 315–331.
37. Tu, Y.F.; Chien, C.S.; Yarmishyn, A.A.; Lin, Y.Y.; Luo, Y.H.; Lin, Y.T.; et al. "A Review of SARS-CoV-2 and the Ongoing Clinical Trials." **Int J Mol Sci** 2020, 21(7), 2657.
38. Ashburn, T.T.; Thor, K.B. "Drug Repositioning: Identifying and Developing New Uses for Existing Drugs." **Nat. Rev. Drug Discov.** 2004, 3(8), 673–683.
39. Pushpakom, S.; Iorio, F.; Eyers, P. A.; Escott, K.J.; Hopper, S.; Wells, A.; et al. "Drug Repurposing: Progress, Challenges and Recommendations." **Nat. Rev. Drug Discov.** 2018, 18, 41–58.
40. Mani, D.; Wadhvani, A.; Krishnamurthy, P.T. "Drug Repurposing in Antiviral Research: A Current Scenario." **J. Young Pharm.** 2019, 11, 117–121.
41. Viveiros Rosa, S.G.; Santos, W.C. "Clinical Trials on Drug Repositioning for COVID-19 Treatment." **Rev. Panam. Salud Publica** 2020, 44, e40.
42. Cao, B.; Wang, Y.; Wen, D.; Liu, W.; Wang, J.; Fan, G.; et al. "A Trial of Lopinavir–Ritonavir in Adults Hospitalized with Severe Covid-19." **N. Engl. J. Med.** 2020, 382, 1787–1799.

43. Bolcato, G.; Bissaro, M.; Pavan, M.; Sturlese, M.; Moro, S. “Targeting the Coronavirus SARS-CoV-2: Computational Insights into the Mechanism of Action of the Protease Inhibitors Lopinavir, Ritonavir and Nelfinavir.” **Sci. Rep.** 2020, 10, 20927.
44. Gautret, P.; Lagier, J.C.; Parola, P.; Meddeb, L.; Mailhe, M.; Doudier, B.; et al. “Hydroxychloroquine and Azithromycin as a Treatment of COVID-19: Results of an Open-Label Non-Randomized Clinical Trial.” **Int. J. Antimicrob. Agents** 2020, 56(1), 105–949.
45. Arshad, S.; Kilgore, P.; Chaudhry, Z.S.; Jacobsen, G.; Wang, D.D.; Huitsing, K.; et al. “Treatment with Hydroxychloroquine, Azithromycin, and Combination in Patients Hospitalized with COVID-19.” **Int. J. Infect. Dis.** 2020, 97, 396–403.
46. The RECOVERY Collaborative Group. “Dexamethasone in Hospitalized Patients with Covid-19.” **N. Engl. J. Med.** 2021, 384, 693–704.
47. Tang, N.; Bai, H.; Chen, X.; Gong, J.; Li, D.; Sun, Z. “Anticoagulant Treatment is Associated with Decreased Mortality in Severe Coronavirus Disease 2019 Patients with Coagulopathy.” **J. Thromb. Haemost.** 2020, 18, 1094–1099.
48. Giamarellos-Bourboulis, E.J.; Netea, M.G.; Rovina, N.; Akinosoglou, K.; Antoniadou, A.; Antonakos, N.; et al. “Complex Immune Dysregulation in COVID-19 Patients with Severe Respiratory Failure.” **Cell. Host. Microbe** 2020, 27, 992–1000.
49. Moore, J.B.; June, C.H. “Cytokine Release Syndrome in Severe COVID-19.” **Science** 2020, 368(6490), 473–474 (2020).
50. Xu, X.; Han, M.; Li, T.; Sun, W.; Wang, D.; Fu, B.; et al. “Effective Treatment of Severe COVID-19 Patients with Tocilizumab.” **Proc. Natl. Acad. Sci.** 2020, 117, 10970–10975.
51. Gordon, A.C.; Mouncey, P.R.; Al-Beidh, F.; Rowan, K.M.; Nichol, A.D.; Arabi, Y.M.; “Interleukin-6 Receptor Antagonists in Critically Ill Patients with Covid-19.” **N. Engl. J. Med.** 2021, 384, 1491–1502.
52. Cavalli, G.; De Luca, G.; Campochiaro, C.; Della-Torre, E.; Ripa, M.; Canetti, D.; et al. “Interleukin-1 Blockade with High-Dose Anakinra in Patients with COVID-19, Acute Respiratory Distress Syndrome, and Hyperinflammation: A Retrospective Cohort Study.” **Lancet Rheumatol.** 2020, 2, e325–e331.
53. Marconi, V.C.; Ramanan, A.V.; de Bono, S.; Kartman, C.E.; Krishnan, V.; Liao, R.; et al. “Efficacy and Safety of Baricitinib for the Treatment of Hospitalised Adults with COVID-19 (COV-BARRIER): A Randomised, Double-Blind, Parallel-Group, Placebo-Controlled Phase 3 Trial.” **Lancet Respir. Med.** 2021, 9, 1407–1418.

54. Kalil, A.C.; Patterson, T.F.; Mehta, A.K.; Tomashek, K.M.; Wolfe, C.R.; Ghazaryan, V.; et al. “Baricitinib plus Remdesivir for Hospitalized Adults with Covid-19.” **N. Engl. J. Med.** 2021, 384, 795–807.
55. Rubin, D.; Chan-Tack, K.; Farley, J.; Sherwat, A. “FDA Approval of Remdesivir — A Step in the Right Direction.” **N. Engl. J. Med.** 2020, 383, 2598–2600.
56. Malin, J.J.; Suárez, I.; Priesner, V.; Fätkenheuer, G.; Rybniker, J. “Remdesivir against COVID-19 and Other Viral Diseases.” **Clin. Microbiol. Rev.** 2021, 34, 1–21.
57. Beigel, J.H.; Tomashek, K.M.; Dodd, L.E.; Mehta, A.K.; Zingman, B.S.; Kalil, A.C.; et al. “Remdesivir for the Treatment of Covid-19 — Final Report.” **N. Engl. J. Med.** 2020, 383, 1813–1826 (2020).
58. Chen, L.; Xiong, J.; Bao, L.; Shi, Y. “Convalescent Plasma as a Potential Therapy for COVID-19.” **Lancet Infect. Dis.** 2020, 20, 398–400.
59. World Health Organization. Use of Convalescent Whole Blood or Plasma Collected from Patients Recovered from Ebola Virus Disease for Transfusion, as an Empirical Treatment During Outbreaks: Interim Guidance for National Health Authorities and Blood Transfusion Services. World Health Organization; 2014 (No. WHO/HIS/SDS/2014.8).
60. Arabi, Y.; Balkhy, H.; Hajeer, A.H.; Bouchama, A.; Hayden, F.G.; Al-Omari, A.; et al. “Feasibility, Safety, Clinical, and Laboratory Effects of Convalescent Plasma Therapy for Patients with Middle East Respiratory Syndrome Coronavirus Infection: A Study Protocol.” **Springerplus** 2015, 4(1), 1–8.
61. Duan, K.; Liu, B.; Li, C.; Zhang, H.; Yu, T.; Qu, J.; et al. “Effectiveness of Convalescent Plasma Therapy in Severe COVID-19 Patients.” **Proc. Natl. Acad. Sci. USA** 2020, 117, 9490–9496.
62. Li, L.; Zhang, W.; Hu, Y.; Tong, X.; Zheng, S.; Yang, J.; et al. “Effect of Convalescent Plasma Therapy on Time to Clinical Improvement in Patients with Severe and Life-threatening COVID-19: A Randomized Clinical Trial.” **JAMA** 2020, 324, 460–470.
63. Simonovich, V.A.; Burgos Pratx, L.D.; Scibona, P.; Beruto, M.V.; Vallone, M.G.; Vázquez, C.; et al. “A Randomized Trial of Convalescent Plasma in Covid-19 Severe Pneumonia.” **N. Engl. J. Med.** 2021, 384, 619–629.
64. Pinto, D.; Park, Y.J.; Beltramello, M.; Walls, A.C.; Tortorici, M.A.; Bianchi, S.; et al. “Cross-neutralization of SARS-CoV-2 by a Human Monoclonal SARS-CoV Antibody.” **Nature** 2020, 583, 290–295.
65. Tian, X.; Li, C.; Huang, A.; Xia, S.; Lu, S.; Shi, Z.; et al. “Potent Binding of 2019 Novel Coronavirus Spike Protein by a SARS Coronavirus-specific Human Monoclonal Antibody.” **Emerg. Microbes Infect.** 2020, 9, 382–385.

66. AIFA. Italian Medicines Agency “Use of monoclonal antibodies for COVID-19 | Italian Medicines Agency. <https://www.aifa.gov.it/en/uso-degli-anticorpi-monoclonali> (Accessed on 25 October 2023).
67. Corti, D.; Purcell, L.A.; Snell, G.; Veessler, D. “Tackling COVID-19 with Neutralizing Monoclonal Antibodies.” **Cell** 2021, 184, 3086–3108.
68. Kaplon, H.; Reichert, J.M. “Antibodies to Watch in 2021.” **MAbs** 2021, 13, 1860476.
69. Kaplon, H.; Chenoweth, A.; Crescioli, S.; Reichert, J.M. “Antibodies to Watch in 2022.” **MAbs** 2022, 14, 2014296.
70. Zost, S.J.; Gilchuk, P.; Case, J.B.; Binshtein, E.; Chen, R.E.; Nkolola, J.P., et al. “Potently neutralizing and protective human antibodies against SARS-CoV-2.” **Nature** 2020, 584, 443–449.
71. Le, T.T.; Andreadakis, Z.; Kumar, A.; Román, R.G.; Tollefsen, S.; Saville, M.; Mayhew, S. et al. “The COVID-19 Vaccine Development Landscape.” **Nat. Rev. Drug Discov.** 2020, 19(5), 305–306.
72. Kashte, S.; Gulbake, A.; El-Amin, S.F.; Gupta, A. “COVID-19 Vaccines: Rapid Development, Implications, Challenges and Future Prospects.” **Hum. Cell.** 2021, 34, 711–733.
73. Pollard, A.J.; Bijker, E.M. “A Guide to Vaccinology: From Basic Principles to new Developments.” **Nat. Rev. Immunol.** 2021, 21, 83–100.
74. Mascellino, M.T.; di Timoteo, F.; de Angelis, M.; Oliva, A. “Overview of the Main Anti-SARS-CoV-2 Vaccines: Mechanism of Action, Efficacy and Safety.” **Infect. Drug Resist.** 2021, 14, 3459–3476.
75. Doroftei, B.; Ciobica, A.; Ilie, O.D.; Maftai, R.; Ilea, C. “Mini-review Discussing the Reliability and Efficiency of Covid-19 Vaccines.” **Diagnostics** 2021, 11(4), 579.
76. Jara, A.; Undurraga, E.A.; González, C.; Paredes, F.; Fontecilla, T.; Jara, G.; et al. “Effectiveness of an Inactivated SARS-CoV-2 Vaccine in Chile.” **N. Engl. J. Med.** 2021, 385, 875–884.
77. Tanriover, M.D.; Doğanay, H.L.; Akova, M.; Güner, H.R.; Azap, A.; Akhan, S.; et al. “Efficacy and Safety of an Inactivated Whole-virion SARS-CoV-2 Vaccine (CoronaVac): Interim Results of a Double-blind, Randomised, Placebo-Controlled, Phase 3 Trial in Turkey.” **Lancet** 2021, 398, 213–222.
78. Polack, F.P.; Thomas, S.J.; Kitchin, N.; Absalon, J.; Gurtman, A.; Lockhart, S.; et al. Safety and Efficacy of the BNT162b2 mRNA Covid-19 Vaccine.” **N. Engl. J. Med.** 2020, 383, 2603–2615.

79. Baden, L.R.; El Sahly, H.M.; Essink, B.; Kotloff, K.; Frey, S.; Novak, R.; et al. “Efficacy and Safety of the mRNA-1273 SARS-CoV-2 Vaccine.” **N. Engl. J. Med.** 2021, 384, 403–416.
80. Li, Q.; Wu, J.; Nie, J.; Zhang, L.; Hao, H.; Liu, S.; et al. “The Impact of Mutations in SARS-CoV-2 Spike on Viral Infectivity and Antigenicity.” **Cell** 2020, 182, 1284.
81. Harvey, W.T.; Carabelli, A.M.; Jackson, B.; Gupta, R.K.; Thomson, E.C.; Harrison, E.M.; et al. “SARS-CoV-2 Variants, Spike Mutations and Immune Escape.” **Nat. Rev. Microbiol.** 2021, 19, 409–424.
82. Forster, P.; Forster, L.; Renfrew, C.; Forster, M. “Phylogenetic Network Analysis of SARS-CoV-2 Genomes.” **Proc. Natl. Acad. Sci. USA** 2020, 117, 9241–9243.
83. Oran, D.P.; Topol, E.J. “Prevalence of Asymptomatic SARS-CoV-2 Infection.” **Ann. Inter. Med.** 2020, 173, 362–368.
84. Hellewell, J.; Abbott, S.; Gimma, A.; Bosse, N.I.; Jarvis, C.I.; Russell, T.W., et al. “Feasibility of Controlling COVID-19 Outbreaks by Isolation of Cases and Contacts.” **Lancet Glob. Health** 2020, 8, e488–e496.
85. Garcia-Beltran, W.F.; Lam, E.C.; Denis, K.S.; Nitido, A.D.; Garcia, Z.H.; Hauser, B.M.; et al. “Multiple SARS-CoV-2 Variants Escape Neutralization by vaccine-Induced Humoral Immunity.” **Cell** 2021, 184, 2372–2383.
86. Fiolet, T.; Kherabi, Y.; MacDonald, C.J.; Ghosn, J.; Peiffer-Smadja, N. “Comparing COVID-19 Vaccines for their Characteristics, Efficacy and Effectiveness against SARS-CoV-2 and Variants of Concern: A Narrative Review.” **Clin. Microbiol. Infect.** 2022, 28, 202–221.
87. Randolph, H.E.; Barreiro, L.B. “Herd Immunity: Understanding COVID-19.” **Immunity** 2020, 52, 737–741.
88. Mathieu, E.; Ritchie, H.; Ortiz-Ospina, E.; Roser, M.; Hasell, J.; Appel, C.; et al. “A global database of COVID-19 vaccinations.” **Nat. Hum. Behav.** 2021, 5, 947–953.
89. Aksamentov, I.; Roemer, C.; Hodcroft, E.B.; Neher, R.A. “Nextclade: Clade Assignment, Mutation Calling and Quality Control for Viral Genomes.” **J. Open Source Softw.** 2021, 6, 3773.
90. World Health Organization. “Tracking SARS-CoV-2 variants. <https://www.who.int/activities/tracking-SARS-CoV-2-variants> (Accessed on 25 October 2023).
91. Frampton, D.; Rampling, T.; Cross, A.; Bailey, H.; Heaney, J.; Byott, M.; et al. “Genomic Characteristics and Clinical Effect of the Emergent SARS-CoV-2 B.1.1.7

- Lineage in London, UK: A Whole-genome Sequencing and Hospital-based Cohort Study.” **Lancet Infect. Dis.** 2021, 21, 1246.
92. Campbell, F.; Archer, B.; Laurenson-Schafer, H.; Jinnai, Y.; Konings, F.; Batra, N.; et al. “Increased Transmissibility and Global Spread of SARSCoV- 2 Variants of Concern as at June 2021.” **Eurosurveillance** 2021, 26, 1–6.
  93. Davies, N.G.; Abbott, S.; Barnard, R.C.; Jarvis, C.I.; Kucharski, A.J.; Munday, J.D.; et al. “Estimated Transmissibility and Impact of SARS-CoV-2 lineage B.1.1.7 in England.” **Science** 2021, 372(6538), eabg3055.
  94. Volz, E.; Mishra, S.; Chand, M.; Barrett, J.C.; Johnson, R.; Geidelberg, L.; et al. “Assessing Transmissibility of SARS-CoV-2 lineage B.1.1.7 in England.” **Nature** 2021, 593, 266–269.
  95. Collier, D.A.; De Marco, A.; Ferreira, I.A.; Meng, B.; Datir, R.P.; Walls, A.C.; et al. “Sensitivity of SARS-CoV-2 B.1.1.7 to mRNA Vaccine-elicited Antibodies.” **Nature** 2021, 593, 136–141.
  96. Chen, R.E.; Zhang, X.; Case, J.B.; Winkler, E.S.; Liu, Y.; VanBlargan, L.A.; et al. “Resistance of SARS-CoV-2 Variants to Neutralization by Monoclonal and Serum-derived Polyclonal Antibodies.” **Nat. Med.** 2021, 27, 717–726.
  97. Wang, P.; Nair, M.S.; Liu, L.; Iketani, S.; Luo, Y.; Guo, Y.; et al. “Antibody resistance of SARS-CoV-2 Variants B.1.351 and B.1.1.7.” **Nature** 2021, 593, 130–135.
  98. Haas, E.J.; Angulo, F.J.; McLaughlin, J.M.; Anis, E.; Singer, S.R.; Khan, F.; et al. “Impact and Effectiveness of mRNA BNT162b2 Vaccine against SARS-CoV-2 Infections and COVID-19 Cases, Hospitalisations, and Deaths Following a Nationwide Vaccination Campaign in Israel: An Observational Study Using National Surveillance Data.” **Lancet** 2021, 397, 1819–1829.
  99. Lopez Bernal, J.; Andrews, N.; Gower, C.; Gallagher, E.; Simmons, R.; Thelwall, S.; et al. Effectiveness of Covid-19 Vaccines against the B.1.617.2 (Delta) Variant.” **N. Engl. J. Med.** 2021, 385, 585–594.
  100. Planas, D.; Veyer, D.; Baidaliuk, A.; Staropoli, I.; Guivel-Benhassine, F.; Rajah, M.M.; et al. “Reduced Sensitivity of SARS-CoV-2 Variant Delta to Antibody Neutralization.” **Nature** 2021, 596, 276–280.
  101. Liu, C.; Ginn, H.M.; Dejnirattisai, W.; Supasa, P.; Wang, B.; Tuekprakhon, A.; et al. “Reduced Neutralization of SARS-CoV-2 B.1.617 by Vaccine and Convalescent Serum.” **Cell** 2021, 184, 4220–4236.
  102. Mlcochova, P.; Kemp, S.A.; Dhar, M.S.; Papa, G.; Meng, B.; Ferreira, I.A.; et al. “SARS-CoV-2 B.1.617.2 Delta Variant Replication and Immune Evasion.” **Nature** 2021, 599(7883), 114–119.



103. Twohig, K.A.; Nyberg, T.; Zaidi, A.; Thelwall, S.; Sinnathamby, M.A.; Aliabadi, S.; et al. “Hospital Admission and Emergency Care Attendance Risk for SARS-CoV-2 Delta (B.1.617.2) Compared with Alpha (B.1.1.7) Variants of Concern: A Cohort Study.” **Lancet Infect. Dis.** 2022, 22, 35–42.
104. Gao, S.J.; Guo, H.; Luo, G. “Omicron Variant (B.1.1.529) of SARS-CoV-2, a Global Urgent Public Health Alert!” **J. Med. Virol.** 2022, 94, 1255–1256.
105. Araf, Y.; Akter, F.; Tang, Y.D.; Fatemi, R.; Parvez, M.S.A.; Zheng, C.; Hossain, M.G. “Omicron Variant of SARS-CoV-2: Genomics, Transmissibility, and Responses to Current COVID-19 Vaccines.” **J. Med. Virol.** 2022, 94, 1825–1832.
106. Liu, L.; Iketani, S.; Guo, Y.; Chan, J.F.W.; Wang, M.; Liu, L.; et al. “Striking Antibody Evasion Manifested by the Omicron Variant of SARS-CoV-2.” **Nature** 2022, 602, 676–681.
107. Dejnirattisai, W.; Shaw, R.H.; Supasa, P.; Liu, C.; Stuart, A.S.; Pollard, A.J.; et al. “Reduced Neutralisation of SARS-CoV-2 Omicron B.1.1.529 Variant by Post-immunisation Serum.” **Lancet** 2022, 399, 234–236.
108. Cao, Y.; Wang, J.; Jian, F.; Xiao, T.; Song, W.; Yisimayi, A.; Xie, X.S. “Omicron Escapes the Majority of Existing SARS-CoV-2 Neutralizing Antibodies.” **Nature** 2022, 602, 657–663.
109. Hoffmann, M.; Krüger, N.; Schulz, S.; Cossmann, A.; Rocha, C.; Kempf, A.; et al. “The Omicron Variant is Highly Resistant against Antibody-mediated neutralization: Implications for Control of the COVID-19 Pandemic.” **Cell** 2022, 185, 447–456.
110. Nemet, I.; Kliker, L.; Lustig, Y.; Zuckerman, N.; Erster, O.; Cohen, C.; et al. “Third BNT162b2 Vaccination Neutralization of SARS-CoV-2 Omicron Infection.” **N. Engl. J. Med.** 2022, 386, 492–494.
111. Dhawan, M.; Saied, A.A.; Mitra, S.; Alhumaydhi, F.A.; Emran, T.B.; Wilairatana, P. “Omicron Variant (B.1.1.529) and its Sublineages: What Do We Know so far amid the Emergence of Recombinant Variants of SARS-CoV-2?” **Biomed. Pharmacother.** 2022, 154, 113522.
112. Ou, J.; Lan, W.; Wu, X.; Zhao, T.; Duan, B.; Yang, P.; et al. “Tracking SARS-CoV-2 Omicron Diverse Spike Gene Mutations Identifies Multiple Inter-variant Recombination Events.” **Signal. Transduct. Target Ther.** 2022, 7(1), 138.
113. Kimura, I.; Yamasoba, D.; Tamura, T.; Nao, N.; Suzuki, T.; Oda, Y.; et al. “Virological Characteristics of the SARS-CoV-2 Omicron BA.2 Subvariants, Including BA.4 and BA.5.” **Cell** 2022, 185, 3992–4007.
114. Wilhelm, A.; Widera, M.; Grikscheit, K.; Toptan, T.; Schenk, B.; Pallas, C.; et al. “Limited Neutralisation of the SARS-CoV-2 Omicron Subvariants BA.1 and BA.2



- by Convalescent and Vaccine Serum and Monoclonal Antibodies.” **EBioMedicine** 2022, 82, 104158.
115. Arora, P.; Zhang, L.; Rocha, C.; Sidarovich, A.; Kempf, A.; Schulz, S.; et al. “Comparable Neutralisation Evasion of SARS-CoV-2 Omicron Subvariants BA.1, BA.2, and BA.3.” **Lancet Infect. Dis.** 2022, 22, 766–767.
  116. Evans, J.P.; Zeng, C.; Qu, P.; Faraone, J.; Zheng, Y.M.; Carlin, C.; et al. “Neutralization of SARS-CoV-2 Omicron sub-lineages BA.1, BA.1.1, and BA.2.” **Cell. Host Microbe** 2022, 30, 1093–1102.
  117. Hachmann, N.P.; Miller, J.; Collier, A.R.Y.; Ventura, J.D.; Yu, J.; Rowe, M.; et al. “Neutralization Escape by SARS-CoV-2 Omicron Subvariants BA.2.12.1, BA.4, and BA.5.” **N. Engl. J. Med.** 2022, 387, 86–88.
  118. Arora, P.; Kempf, A.; Nehlmeier, I.; Schulz, S.R.; Cossmann, A.; Stankov, M.V.; et al. “Augmented Neutralisation Resistance of Emerging Omicron Subvariants BA.2.12.1, BA.4, and BA.5.” **Lancet Infect. Dis.** 2022, 22, 1117–1118.
  119. Wang, Q.; Guo, Y.; Iketani, S.; Nair, M.S.; Li, Z.; Mohri, H.; et al. “Antibody evasion by SARS-CoV-2 Omicron Subvariants BA.2.12.1, BA.4 and BA.5.” **Nature** 2022, 608, 603–608.
  120. Walls, A.C.; Park, Y.J.; Tortorici, M.A.; Wall, A.; McGuire, A.T.; Velesler, D. “Structure, Function, and Antigenicity of the SARS-CoV-2 Spike Glycoprotein.” **Cell** 2020, 181, 281–292.
  121. Gadanec, L.K.; McSweeney, K.R.; Qaradakhi, T.; Ali, B.; Zulli, A.; Apostolopoulos, V. “Can SARS-CoV-2 Virus Use Multiple Receptors to Enter Host Cells?” **Int. J. Mol. Sci.** 2021, 22(3), 992.
  122. Shen, S.; Zhang, J.; Fang, Y.; Lu, S.; Wu, J.; Zheng, X.; Deng, F. “SARS-CoV-2 Interacts with Platelets and Megakaryocytes via ACE2-independent Mechanism.” **J. Hematol. Oncol.** 2021, 14(1), 1–5.
  123. Hoffmann, M.; Kleine-Weber, H.; Schroeder, S.; Krüger, N.; Herrler, T.; Erichsen, S.; et al. “SARS-CoV-2 Cell Entry Depends on ACE2 and TMPRSS2 and Is Blocked by a Clinically Proven Protease Inhibitor.” **Cell** 2020, 181, 271–280.e8.
  124. Hamming, I.; Timens, W.; Bulthuis, M.L.C.; Lely, A.T.; Navis, G.V.; van Goor, H. “Tissue Distribution of ACE2 Protein, the Functional Receptor for SARS Coronavirus. A First Step in Understanding SARS Pathogenesis.” **J. Pathol.** 2004, 203, 631–637.
  125. Glowacka, I.; Bertram, S.; Müller, M.A.; Allen, P.; Soilleux, E.; Pfefferle, S.; et al. “Evidence that TMPRSS2 Activates the Severe Acute Respiratory Syndrome

- Coronavirus Spike Protein for Membrane Fusion and Reduces Viral Control by the Humoral Immune Response.” **J. Virol.** 2011, 85, 4122–4134.
126. Belouzard, S.; Millet, J.K.; Licitra, B.N.; Whittaker, G.R. “Mechanisms of Coronavirus Cell Entry Mediated by the Viral Spike Protein.” **Viruses** 2012, 4, 1011–1033.
  127. Hoffmann, M.; Kleine-Weber, H.; Pöhlmann, S.A “Multibasic Cleavage Site in the Spike Protein of SARS-CoV-2 Is Essential for Infection of Human Lung Cells.” **Mol. Cell.** 2020, 78, 779–784.
  128. Wrapp, D.; Wang, N.; Corbett, K.S.; Goldsmith, J.A.; Hsieh, C.L.; Abiona, O.; et al. “Cryo-EM Structure of the 2019-nCoV Spike in the Prefusion Conformation.” **Science** 2020, 367(6483), 1260–1263.
  129. Guillén, J.; Pérez-Berná, A.J.; Moreno, M.R.; Villalain, J. “Identification of the Membrane-active Regions of the Severe Acute Respiratory Syndrome Coronavirus Spike Membrane Glycoprotein using a 16/18-mer Peptide Scan: Implications for the Viral Fusion Mechanism.” **J. Virol.** 2005, 79, 1743–1752.
  130. Zhu, C.; He, G.; Yin, Q.; Zeng, L.; Ye, X.; Shi, Y.; Xu, W. “Molecular Biology of the SARs-CoV-2 Spike Protein: A Review of Current Knowledge.” **J. Med. Virol.** 2021, 93, 5729–5741.
  131. Yan, R.; Zhang, Y.; Li, Y.; Xia, L.; Guo, Y.; Zhou, Q. “Structural Basis for the Recognition of SARS-CoV-2 by Full-length Human ACE2.” **Science** 2020, 367(6485), 1444–1448.
  132. Huang, Y.; Yang, C.; Xu, X.F.; Xu, W.; Liu, S.W. “Structural and functional properties of SARS-CoV-2 Spike Protein: Potential Antivirus Drug Development for COVID-19.” **Acta Pharmacol. Sin.** 2020, 41, 1141–1149.
  133. Schroth-Diez, B.; Ludwig, K.; Baljinnyam, B.; Kozerski, C.; Huang, Q.; Herrmann, A. “The Role of the Transmembrane and of the Intraviral Domain of Glycoproteins in Membrane Fusion of Enveloped Viruses.” **Biosci. Rep.** 2000, 20, 571–595.
  134. Reuven, E.M.; Dadon, Y.; Viard, M.; Manukovsky, N.; Blumenthal, R.; Shai, Y. “HIV-1 gp41 Transmembrane Domain Interacts with the Fusion Peptide: Implication in Lipid Mixing and Inhibition of Virus-cell Fusion.” **Biochemistry** 2012, 51, 2867–2878.
  135. Petit, C.M.; Melancon, J.M.; Chouljenko, V.N.; Colgrove, R.; Farzan, M.; Knipe, D.M.; Kousoulas, K.G. “Genetic Analysis of the SARS-coronavirus Spike Glycoprotein Functional Domains Involved in Cell-surface Expression and Cell-to-cell Fusion.” **Virology** 2005, 341, 215–230.

136. Li, F. "Structure, Function, and Evolution of Coronavirus Spike Proteins." **Annu. Rev. Virol.** 2016, 3, 237–261.
137. Hu, Q.; Xiong, Y.; Zhu, G.H.; Zhang, Y.N.; Zhang, Y.W.; Huang, P.; Ge, G.B. "The SARS-CoV-2 main protease (M(pro)): Structure, Function, and Emerging Therapies for COVID-19." **MedComm.** 2022, 3, e151.
138. Tyndall, J.D.A. "S-217622, a 3CL Protease Inhibitor and Clinical Candidate for SARS-CoV-2." **J. Med. Chem.** 2022, 65, 6496–6498.
139. Unoh, Y.; Uehara, S.; Nakahara, K.; Nobori, H.; Yamatsu, Y.; Yamamoto, S.; et al. "Discovery of S-217622, a Noncovalent Oral SARS-CoV-2 3CL Protease Inhibitor Clinical Candidate for Treating COVID-19." **J. Med. Chem.** 2022, 65, 6499–6512.
140. Neamati, N. "Advances toward COVID-19 Therapies Special Issue." **J. Med. Chem.** 2022, 65, 2713–2715.
141. McDonald, J.T.; Enguita, F.J.; Taylor, D.; Griffin, R.J.; Priebe, W.; Emmett, M.R.; et al. "Role of miR-2392 in Driving SARS-CoV-2 Infection." **Cell. Rep.** 2021, 37, 109839.
142. McCollum, C.R.; Courtney, C.M.; O'Connor, N.J.; Aunins, T.R.; Ding, Y.; Jordan, T.X.; et al. "Nanoligomers Targeting Human miRNA for the Treatment of Severe COVID-19 are Safe and Nontoxic in Mice." **ACS Biomater. Sci. Eng.** 2022, 8, 3087–3106.
143. Smith, C.D.; Maines, L.W.; Keller, S.N.; Katz Ben-Yair, V.; Fathi, R.; Plasse, T.F.; Levitt, M.L. Recent Progress in the Development of Opananib for the Treatment of COVID-19." **Drug Des. Devel. Ther.** 2022, 16, 2199–2211.
144. Qin, G.; Zhao, C.; Liu, Y.; Zhang, C.; Yang, G.; Yang, J.; et al. "RNA G-quadruplex Formed in SARS-CoV-2 Used for COVID-19 Treatment in Animal Models." **Cell Discov.** 2022, 8, 86.
145. Ceramella, J.; Iacopetta, D.; Sinicropi, M.S.; Andreu, I.; Mariconda, A.; Saturnino, C.; et al. "Drugs for COVID-19: An Update." **Molecules** 2022, 27, 8562.
146. Anighoro, A.; Bajorath, J.; Rastelli, G. "Polypharmacology: Challenges and Opportunities in Drug Discovery." **J. Med. Chem.** 2014, 57, 7874–7887.
147. Peters, J.U. "Polypharmacology - Foe or Friend?" **J. Med. Chem.** 2013, 56, 8955–8971.
148. Reddy, A.S.; Zhang, S. "Polypharmacology: Drug discovery for the future." **Expert Rev. Clin. Pharmacol.** 2013, 6, 41–47.
149. Nasab, M.G.; Saghadzadeh, A.; Rezaei, N. "SARS-CoV-2-A Tough Opponent for the Immune System." **Arch. Med. Res.** 2020, 51, 589–592.

150. Gordon, A.C.; Mouncey, P.R.; Al-Beidh, F.; Rowan, K.M.; Nichol, A.D.; Arabi, Y.M.; D.E.; Jang, G.M.; Bouhaddou, M.; Xu, J.; Obernier, K.; White, K.M.; et al. “A SARS-CoV-2 Protein Interaction Map Reveals Targets for Drug Repurposing.” **Nature** 2020, 583(7816), 459–468.
151. Lubin, J.H.; Zardecki, C.; Dolan, E.M.; Lu, C.; Shen, Z.; Dutta, S.; et al. “Evolution of the SARS-CoV-2 proteome in three dimensions (3D) during the first 6 months of the COVID-19 pandemic.” **Proteins** 2022, 90, 1054–1080.
152. Osipiuk, J.; Azizi, S.A.; Dvorkin, S.; Endres, M.; Jedrzejczak, R.; Jones, K.A.; et al. “Structure of Papain-like Protease from SARS-CoV-2 and its Complexes with Non-covalent Inhibitors.” **Nat. Commun.** 2021, 12(1), 743.
153. Rut, W.; Lv, Z.; Zmudzinski, M.; Patchett, S.; Nayak, D.; Snipas, S.J.; et al. “Activity Profiling and Crystal Structures of Inhibitor-bound SARS-CoV-2 Papain-like Protease: A Framework for Anti-COVID-19 Drug Design.” **Sci. Adv.** 2020, 6, 4596–4612.
154. Klemm, T.; Ebert, G.; Calleja, D.J.; Allison, C.C.; Richardson, L.W.; Bernardini, J.P., et al. “Mechanism and Inhibition of the Papain-like Protease, PLpro, of SARS-CoV-2.” **EMBO J.** 2020, 39, e106275.
155. Shin, D.; Mukherjee, R.; Grewe, D.; Bojkova, D.; Baek, K.; Bhattacharya, A.; et al. “Papain-like Protease Regulates SARS-CoV-2 Viral Spread and Innate Immunity.” **Nature** 2020, 587(7835), 657–662.
156. Gao, Y.; Yan, L.; Huang, Y.; Liu, F.; Zhao, Y.; Cao, L.; et al. “Structure of the RNA-dependent RNA Polymerase from COVID-19 Virus.” **Science** 2020, 368(6492), 779–782.
157. Kim, D.; Lee, J.Y.; Yang, J.S.; Kim, J.W.; Kim, V.N.; Chang, H. “The Architecture of SARS-CoV-2 Transcriptome.” **Cell** 2020, 181, 914–921.
158. Hillen, H.S.; Kokic, G.; Farnung, L.; Dienemann, C.; Tegunov, D.; Cramer, P. “Structure of Replicating SARS-CoV-2 Polymerase.” **Nature** 2020, 584, 154–156.
159. Wang, Q.; Wu, J.; Wang, H.; Gao, Y.; Liu, Q.; Mu, A.; et al. “Structural Basis for RNA Replication by the SARS-CoV-2 Polymerase.” **Cell** 2020, 182, 417–428.
160. Yin, W.; Mao, C.; Luan, X.; Shen, D.D.; Shen, Q.; Su, H.; et al. “Structural Basis for Inhibition of the RNA-dependent RNA Polymerase from SARS-CoV-2 by Remdesivir.” **Science** 2020, 368(6498), 1499–1504.
161. Kokic, G.; Hillen, H.S.; Tegunov, D.; Dienemann, C.; Seitz, F.; Schmitzova, J.; et al. “Mechanism of SARS-CoV-2 Polymerase Stalling by Remdesivir.” **Nat. Commun.** 2021, 12, 1–7.

162. Chen, J.; Malone, B.; Llewellyn, E.; Grasso, M.; Shelton, P.M.; Olinares, P.D.B.; et al. “Structural Basis for Helicase-Polymerase Coupling in the SARS-CoV-2 Replication-Transcription Complex.” **Cell** 2020, 182, 1560–1573.
163. Awan, F.M.; Yang, B.B.; Naz, A.; Hanif, A.; Ikram, A.; Obaid, A.; et al. “The Emerging Role and Significance of Circular RNAs in Viral Infections and Antiviral Immune Responses: Possible Implication as Theranostic Agents.” **RNA Biol.** 2021, 18(1), 1–15.
164. Adedeji, A.O.; Marchand, B.; Te Velthuis, A.J.; Snijder, E.J.; Weiss, S.; Eoff, R.L.; et al. “Mechanism of Nucleic Acid Unwinding by SARS-CoV Helicase.” **PLoS One** 2012, 7(5), e36521.
165. Mickolajczyk, K.J.; Shelton, P.M.; Grasso, M.; Cao, X.; Warrington, S.E.; Aher, A.; et al. “Force-dependent Stimulation of RNA Unwinding by SARS-CoV-2 nsp13 Helicase.” **Biophys. J.** 2021, 120, 1020–1030.
166. Newman, J.A.; Douangamath, A.; Yadzani, S.; Yosaatmadja, Y.; Aimon, A.; Brandão-Neto, J.; et al. “Structure, Mechanism and Crystallographic Fragment Screening of the SARS-CoV-2 NSP13 Helicase.” **Nat. Commun.** 2021, 12, 4848.
167. Ivanov, K.A.; Thiel, V.; Dobbe, J.C.; Van Der Meer, Y.; Snijder, E.J.; Ziebuhr, J. “Multiple Enzymatic Activities Associated with Severe Acute Respiratory Syndrome Coronavirus Helicase.” **J. Virol.** 2004, 78, 5619–5632.
168. Chen, Y.; Su, C.; Ke, M.; Jin, X.; Xu, L.; Zhang, Z.; et al. “Biochemical and Structural Insights into the Mechanisms of SARS Coronavirus RNA ribose 2’-O-methylation by nsp16/nsp10 Protein Complex.” **PLoS Pathog.** 2011, 7(10), e1002294.
169. Romano, M.; Ruggiero, A.; Squeglia, F.; Maga, G.; Berisio, R.A. “Structural View of SARS-CoV-2 RNA Replication Machinery: RNA Synthesis, Proofreading and Final Capping.” **Cells** 2020, 9(5), 1267.
170. Khailany, R.A.; Safdar, M.; Ozaslan, M. “Genomic Characterization of a Novel SARS-CoV-2.” **Gene Rep.** 2020, 19, 100682.
171. Ogando, N.S.; Zevenhoven-Dobbe, J.C.; van der Meer, Y.; Bredenbeek, P.J.; Posthuma, C.C.; Snijder, E.J. “The Enzymatic Activity of the nsp14 Exoribonuclease Is Critical for Replication of MERS-CoV and SARS-CoV-2.” **J. Virol.** 2020, 94(23).  
Doi: <https://doi.org/10.1128/jvi.01944-20>
172. Ma, Y.; Wu, L.; Shaw, N.; Gao, Y.; Wang, J.; Sun, Y.; et al. “Structural Basis and Functional Analysis of the SARS Coronavirus nsp14-nsp10 Complex.” **Proc. Natl. Acad. Sci. USA** 2015, 112, 9436–9441.
173. Lin, S.; Chen, H.; Chen, Z.; Yang, F.; Ye, F.; Zheng, Y.; et al. “Crystal structure of SARS-CoV-2 nsp10 Bound to nsp14-ExoN Domain Reveals an Exoribonuclease

- with Both Structural and Functional Integrity.” **Nucleic Acids Res.** 2021, 49, 5382–5392.
174. Eckerle, L.D.; Becker, M.M.; Halpin, R.A.; Li, K.; Venter, E.; Lu, X.; et al. “Infidelity of SARS-CoV Nsp14-exonuclease Mutant Virus Replication is Revealed by Complete Genome Sequencing.” **PLoS Pathog.** 2010, 6, 1–15.
  175. Czarna, A.; Plewka, J.; Kresik, L.; Matsuda, A.; Karim, A.; Robinson, C.; et al. “Refolding of Lid Subdomain of SARS-CoV-2 nsp14 upon nsp10 Interaction Releases Exonuclease Activity.” **Structure** 2022, 30, 1050–1054.
  176. Wilamowski, M.; Sherrell, D.A.; Minasov, G.; Kim, Y.; Shuvalova, L.; Lavens, A.; et al. “2'-O methylation of RNA cap in SARS-CoV-2 Captured by Serial Crystallography.” **Proc. Natl. Acad. Sci. USA** 2021, 118, e2100170118.
  177. Lin, S.; Chen, H.; Ye, F.; Chen, Z.; Yang, F.; Zheng, Y.; et al. “Crystal structure of SARS-CoV-2 nsp10/nsp16 2'-O-methylase and its Implication on Antiviral Drug Design.” **Signal Transduct. Target Ther.** 2020, 5(1), 1–4.
  178. Rosas-Lemus, M.; Minasov, G.; Shuvalova, L.; Inniss, N.L.; Kiryukhina, O.; Brunzelle, J.; et al. “High-resolution Structures of the SARS-CoV-2 2'-O-methyltransferase Reveal Strategies for Structure-Based Inhibitor Design.” **Sci. Signal.** 2020, 13, 1202.
  179. Yoshimoto, F.K. “The Proteins of Severe Acute Respiratory Syndrome Coronavirus-2 (SARS CoV-2 or n-COV19), the Cause of COVID-19.” **Protein J.** 2020, 39, 198–216.
  180. Frazier, M.N.; Wilson, I.M.; Krahn, J.M.; Butay, K.J.; Dillard, L.B.; Borgnia, M.J.; et al. “Flipped over U: Structural Basis for dsRNA Cleavage by the SARS-CoV-2 Endoribonuclease.” **Nucleic Acids Res.** 2022, 50, 8290–8301.
  181. Pillon, M.C.; Frazier, M.N.; Dillard, L.B.; Williams, J.G.; Kocaman, S.; Krahn, J.M.; et al. “Cryo-EM structures of the SARS-CoV-2 endoribonuclease Nsp15 reveal insight into nuclease specificity and dynamics.” **Nat. Commun.** 2021, 12(1), 636.
  182. Kim, Y.; Jedrzejczak, R.; Maltseva, N.I.; Wilamowski, M.; Endres, M.; Godzik, A.; et al. “Crystal structure of Nsp15 endoribonuclease NendoU from SARS-CoV-2.” **Protein Sci.** 2020, 29, 1596–1605.
  183. Frazier, M.N.; Dillard, L.B.; Krahn, J.M.; Perera, L.; Williams, J.G.; Wilson, I.M.; et al. “Characterization of SARS2 Nsp15 Nuclease Activity Reveals it’s Mad about U.” **Nucleic Acids Res.** 2021, 49, 10136–10149.
  184. Kim, Y.; Wower, J.; Maltseva, N.; Chang, C.; Jedrzejczak, R.; Wilamowski, M.; et al. “Tipiracil Binds to Uridine Site and Inhibits Nsp15 Endoribonuclease NendoU from SARS-CoV-2.” **Commun. Biol.** 2021, 4(1), 193.

185. Iacopetta, D.; Ceramella, J.; Catalano, A.; Saturnino, C.; Pellegrino, M.; Mariconda, A.; et al. "COVID-19 at a Glance: An Up-to-date Overview on Variants, Drug Design and Therapies." **Viruses** 2022, 14, 573.
186. Anjum, F.; Mohammad, T., Asrani, P., Shafie, A.; Singh, S., Yadav, D.K.; et al. "Identification of Intrinsically Disorder Regions in Non-Structural Proteins of SARS-CoV-2: New Insights into Drug and Vaccine Resistance." **Mol. Cell. Biochem.** 2022, 477(5), 1607–1619.
187. Shamsi, A.; Mohammad, T.; Anwar, S.; AlAjmi, M.F.; Hussain, A.; Rehman, M.T.; et al. "Glecaprevir and Maraviroc are High-Affinity Inhibitors of SARS-CoV-2 Main Protease: Possible Implication in COVID-19 Therapy." **Biosci. Rep.** 2020, 40(6), BSR20201256.
188. Shamsi, A., Mohammad, T.; Anwar, S.; Amani, S.; Khan, M.S.; Husain, F.M., et al. "Potential Drug Targets of SARS-CoV-2: From Genomics to Therapeutics." **Int. J. Biol. Macromol.** 2021, 177, 1–9.
189. Catalano, A.; Iacopetta, D.; Ceramella, J., De Maio, A.C.; Basile, G.; Giuzio, F.; et al. "Are Nutraceuticals Effective in COVID-19 and Post-COVID Prevention and Treatment?" **Foods** 2022, 1(18), 2884.
190. Ceramella, J.; Iacopetta, D.; Sinicropi, M.S.; Andreu, I.; Mariconda, A.; Saturnino, C.; et al. "Drugs for COVID-19: An Update." **Molecules** 2022, 27(23), 8562.
191. Conti, M.; Richter, W.; Mehats, C.; Livera, G.; Park, J.Y.; Jin, C. "Cyclic AMP-specific PDE4 Phosphodiesterases as Critical Components of Cyclic AMP Signaling." **J. Biol. Chem.** 2003, 278(8), 5493–5496.
192. Yan, K.U.O.; Gao, L.N.; Cui, Y.L.; Zhang, Y.I.; Zhou, X.I.N. "The cyclic AMP signaling pathway: Exploring Targets for Successful Drug Discovery." **Mol. Med. Rep.** 2016, 13(5), 3715–3723.
193. Yougbare, I.; Morin, C.; Senouvo, F.Y.; Sirois, C.; Albadin, R., Lugnier, C., Rousseau, E. "NCS 613, a Potent and Specific PDE4 Inhibitor, Displays Anti-Inflammatory Effects on Human Lung Tissues." **Am. J. Physiol. Lung Cell. Mol. Physiol.** 2011, 301, L441–L450.
194. Liu, Z.; Liu, M.; Cao, Z.; Qiu, P.; Song, G. "Phosphodiesterase 4 Inhibitors: A Review of Current Developments (2013–2021)." **Expert Opin. Ther. Pat.** 2022, 32(3), 261–278.
195. Li, H.; Zuo, J.; Tang, W. "Phosphodiesterase-4 Inhibitors for the Treatment of Inflammatory Diseases." **Front. Pharmacol.** 2018, 9, 1048.
196. Zebda, R.; Paller, A.S. "Phosphodiesterase 4 Inhibitors." **J. Am. Acad. Dermatol.** 2018, 78(3), S43–S52.



197. Yang, H.; Wang, J.; Zhang, X.; Zhang, Y.; Qin, Z.L.; Wang, H.; Luo, X.Y. "Application of Topical Phosphodiesterase 4 Inhibitors in Mild to Moderate Atopic Dermatitis: A Systematic Review and Meta-Analysis." **JAMA Dermatol.** 2019, 155(5), 585–593.
198. Ye, W.; Xu, J.P.; Wang, H.T.; Li, X.F.; Wang, W.Y.; Zhou, Z.Z. "Discovery of Novel Trimethoxyphenylbenzo[d]oxazoles as Dual Tubulin/PDE4 Inhibitors Capable of Inducing Apoptosis at G2/M Phase Arrest in Glioma and Lung Cancer Cells." **Eur. J. Med. Chem.** 2021, 224, 113700.
199. Banner, K.H.; Trevethick, M.A. "PDE4 Inhibition: A Novel Approach for the Treatment of Inflammatory Bowel Disease." **Trends Pharmacol. Sci.** 2004, 25(8), 430–436.
200. De Maio, A.C.; Basile, G.; Iacopetta, D.; Catalano, A.; Ceramella, J.; Cafaro, D.; et al. "The Significant Role of Nutraceutical Compounds in Ulcerative Colitis Treatment." **Curr. Med. Chem.** 2022, 29, 4216–4234.
201. Bhat, A.; Ray, B.; Mahalakshmi, A.M.; Tuladhar, S.; Nandakumar, D.N.; Srinivasan, M.; et al. "Phosphodiesterase-4 Enzyme as a Therapeutic Target in Neurological Disorders." **Pharmacol. Res.** 2020, 160, 105078.
202. Ookawara, M.; Nio, Y. "Phosphodiesterase 4 Inhibitors in Diabetic Nephropathy." **Cell. Sign.** 2022, 90, 110185.
203. Lugnier, C.; Al-Kuraishy, H.M.; Rousseau, E. "PDE4 Inhibition as a Therapeutic Strategy for Improvement of Pulmonary Dysfunctions in COVID-19 and Cigarette Smoking." **Biochem. Pharmacol.** 2021, 185, 114431.
204. Mokra, D., Mokry, J. "Phosphodiesterase Inhibitors in Acute Lung Injury: What are the Perspectives?" **Int. J. Mol. Sci.** 2021, 22, 1929.
205. Aragon, I.V.; Boyd, A.; Abou Saleh, L.; Rich, J.; McDonough, W.; Koloteva, A.; et al. "Inhibition of cAMP-phosphodiesterase 4 (PDE4) Potentiates the Anesthetic Effects of Isoflurane in Mice." **Biochem. Pharmacol.** 2021, 186, 114477.
206. Çifci, G.; Aviyente, V.; Akten, E.D. "Molecular Docking Study Based on Pharmacophore Modeling For Novel Phosphodiesterase IV Inhibitors." **Mol. Inform.** 2012, 31(6-7), 459–471.
207. Lugnier, C.; Schoeffter, P.; Le Bec, A.; Strouthou, E.; Stoclet, J.C. "Selective Inhibition of Cyclic Nucleotide Phosphodiesterases of Human, Bovine and Rat Aorta." **Biochem. Pharmacol.** 1986, 35(10), 1743–1751.
208. Crocetti, L.; Floresta, G.; Cilibrizzi, A.; Giovannoni, M.P. "An Overview of PDE4 Inhibitors in Clinical Trials: 2010 to Early 2022." **Molecules** 2022;27(15):4964.



209. Vogel III, E.W.; Morales, F.N.; Meaney, D.F.; Bass, C.R.; Morrison III, B. “Phosphodiesterase-4 Inhibition Restored Hippocampal Long Term Potentiation after Primary Blast.” **Exp. Neurol.** 2017, 293, 91–100.
210. Nguyen, H.O.; Schioppa, T.; Tiberio, L.; Facchinetti, F.; Villetti, G.; Civelli, M.; et al. “The PDE4 Inhibitor Tanimilast Blunts Proinflammatory Dendritic Cell Activation by SARS-CoV-2 ssRNAs.” **Front. Immunol.** 2022, 12, 797390.
211. Paes, D.; Hermans, S.; van den Hove, D.; Vanmierlo, T.; Prickaerts, J.; Carlier, A. “Computational Investigation of the Dynamic Control of cAMP Signaling by PDE4 Isoform Types.” **Biophys. J.** 2022, 121(14), 2693–2711.
212. Boyd, A.; Aragon, I.V.; Rich, J.; McDonough, W.; Oditt, M.; Ireland, D.; et al. “Assessment of PDE4 Inhibitor-Induced Hypothermia as a Correlate of Nausea in Mice.” **Biology** 2021, 10(12), 1355.
213. McDonough, W.; Aragon, I.V.; Rich, J.; Murphy, J.M.; Saleh, L.A.; Boyd, A.; et al. “PAN-Selective Inhibition of cAMP-Phosphodiesterase 4 (PDE4) Induces Gastroparesis in Mice.” **FASEB J.** 2020, 34, 12533–12548.
214. Saleh, L.A.; Boyd, A.; Aragon, I.V.; Koloteva, A.; Spadafora, D.; Mneimneh, W.; et al. “Ablation of PDE4B Protects from *Pseudomonas aeruginosa*-induced acute lung Injury in Mice by Ameliorating the Cytostorm and Associated Hypothermia.” **FASEB J.** 2021, 35, e21797.
215. Azam, M.A.; Tripuraneni, N.S. “Selective Phosphodiesterase 4B Inhibitors: A Review.” **Sci. Pharm.** 2014, 82, 453–481.
216. Angeletti, S.; Benvenuto, D.; Bianchi, M.; Giovanetti, M.; Pascarella, S.; Ciccozzi, M. “COVID-2019: The Role of the nsp2 and nsp3 in its Pathogenesis.” **J. Med. Virol.** 2020, 92, 584–588.
217. Naganuma, K.; Omura, A.; Maekawara, N.; Saitoh, M.; Ohkawa, N.; Kubota, T.; et al. “Discovery of Selective PDE4B Inhibitors.” **Bioorg. Med. Chem. Lett.** 2009, 19, 3174–3176.
218. Gorja, D.R.; Mukherjee, S.; Meda, C.L.T.; Deora, G.S.; Kumar, K.L.; Jain, A.; et al. “Novel N-indolylmethyl Substituted Olanzapine Derivatives: their Design, Synthesis and Evaluation as PDE4B Inhibitors.” **Org. Biomol. Chem.** 2013, 11(13), 2075–2079.
219. Pachetti, M.; Marini, B.; Benedetti, F.; Giudici, F.; Mauro, E.; Storici, P.; et al. “Emerging SARS-CoV-2 Mutation Hot Spots Include a Novel RNA-dependent-RNA Polymerase Variant.” **J. Transl. Med.** 2020, 18, 179.
220. Fox 3rd, D.; Burgin, A.B.; Gurney, M.E. “Structural Basis for the Design of Selective Phosphodiesterase 4B Inhibitors.” **Cell Signal.** 2014, 26, 657–663.

221. Singh, P.; Mishra, M.; Agarwal, S.; Sau, S.; Iyer, A.K.; Kashaw, S.K. "Exploring the Role of Water Molecules in the Ligand Binding Domain of PDE4B and PDE4D: Virtual Screening Based Molecular Docking of Some Active Scaffolds." **Curr. Comp. Aid. Drug Des.** 2019, 15(4), 334–366.
222. Pham, M.T.; Yang, A.J.; Kao, M.S.; Gankhuyag, U.; Zayabaatar, E.; Jin, S.C.; et al. "Gut Probiotic *Lactobacillus rhamnosus* Attenuates PDE4B-Mediated Interleukin-6 Induced by SARS-CoV-2 Membrane Glycoprotein." **J. Nutr. Biochem.** 2021, 98, 108821.
223. Herrmann, F.E.; Hesslinger, C.; Wollin, L.; Nickolaus, P. "BI 1015550 is a PDE4B Inhibitor and a Clinical Drug Candidate for the Oral Treatment of Idiopathic Pulmonary Fibrosis." **Front. Pharmacol.** 2022, 13, 838449.
224. El Tabaa, M.M.; El Tabaa, M.M. "New Putative Insights into Neprilysin (NEP)-Dependent Pharmacotherapeutic Role of Roflumilast in Treating COVID-19." **Eur. J. Pharmacol.** 2020, 889, 173615.
225. Hirose, R.; Manabe, H.; Nonaka, H.; Yanagawa, K.; Akuta, K.; Sato, S.; Ohshima, E.; Ichimura, M. "Correlation between Emetic Effect of Phosphodiesterase 4 Inhibitors and their Occupation of the High-Affinity Rolipram Binding Site in *Suncus murinus* Brain." **Eur. J. Pharmacol.** 2007, 573(1-3), 93–99.
226. Card, G.L.; England, B.P.; Suzuki, Y.; Fong, D.; Powell, B.; Lee, B.; et al. "Structural Basis for the Activity of Drugs that Inhibit Phosphodiesterases." **Structure** 2004, 12, 2233–2247.
227. Trott, O.; Olson, A.J. "AutoDock Vina: Improving the Speed and Accuracy of Docking with a New Scoring Function, Efficient Optimization, and Multithreading." **J. Comput. Chem.** 2010, 31, 455–461.
228. Zhao, Y.; O'Donnell, J.M.; Zhang, H-T. "Inhibitor Binding to Type 4 Phosphodiesterase (PDE4) Assessed using [3H]Piclamilast and [3H]Rolipram." **J. Pharmacol. Exp. Ther.** 2003, 305, 565–572.
229. Tenor, H.; Hedbom, E.; Häuselmann, H.J.; Schudt, C.; Hatzelmann, A. "Phosphodiesterase Isoenzyme Families in Human Osteoarthritis Chondrocytes—Functional Importance of Phosphodiesterase 4." **Br. J. Pharmacol.** 2002, 135(3), 609–618.
230. Kaur, A.; Singh, T.G.; Khan, H.; Kumar, M.; Singh, N.; Abdel-Daim, M.M. "Neuroprotective Effect of Piclamilast-Induced Post-Ischemia Pharmacological Treatment in Mice." **Neurochem. Res.** 2022, 47, 2230–2243.
231. Zhu, J.; Mix, E.; Winblad, B. "The Antidepressant and Antiinflammatory Effects of Rolipram in the Central Nervous System." **CNS Drug. Rev.** 2001, 7(4), 387–398.

232. Varona, S.; Puertas, L.; Galán, M.; Orriols, M.; Cañes, L.; Aguiló, S, et al. “Rolipram Prevents the Formation of Abdominal Aortic Aneurysm (AAA) in Mice: PDE4B as a Target in AAA.” **Antioxidants** 2021, 10, 460.
233. Dong, X.L.; Wang, Y.H.; Xu, J.; Zhang, N. “The Protective Effect of the PDE-4 Inhibitor Rolipram on Intracerebral Haemorrhage Is Associated with the cAMP/AMPK/SIRT1 Pathway.” **Sci. Rep.** 2021, 11(1), 1–10.
234. Qiu, Y.; Yao, J.; Jia, L.; Thompson, D.A.; Zacks, D.N. “Shifting the Balance of Autophagy and Proteasome Activation Reduces Proteotoxic Cell Death: a Novel Therapeutic Approach for Restoring Photoreceptor Homeostasis.” **Cell. Death Dis.** 2019, 10(8), 1–14.
235. Wu, Y.; Li, Z.; Huang, Y.Y.; Wu, D.; Luo, H.B. “Novel Phosphodiesterase Inhibitors for Cognitive Improvement in Alzheimer’s Disease: Miniperspective.” **J. Med. Chem.** 2018, 61(13), 5467–5483.
236. Lan, J.; Ge, J.; Yu, J.; Shan, S.; Zhou, H.; Fan, S. et al. “Structure of the SARS-CoV-2 Spike Receptor-Binding Domain Bound to the ACE2 Receptor.” **Nature** 2020, 581, 215–220.
237. Li, G.; De Clercq, E. “Therapeutic Options for the 2019 Novel Coronavirus (2019-nCoV).” **Nat. Rev. Drug. Discov.** 2020, 19, 149–150.
238. Sanz, R.; Escribano, J.; Pedrosa, M.R.; Aguado, R.; Arnaiz, F.J. Dioxomolybdenum (VI)-Catalyzed Reductive Cyclization of Nitroaromatics. Synthesis of Carbazoles and Indoles.” **Adv. Synth. Catal.** 2007, 349(4,5), 713–718.
239. Saturnino, C.; Palladino, C.; Napoli, M.; Sinicropi, M.S.; Botta, A.; Sala, M.; et al. “Synthesis and Biological Evaluation of New *N*-Alkylcarbazole Derivatives as STAT3 Inhibitors: Preliminary Study.” **Eur. J. Med. Chem.** 2013, 60, 112–119.
240. Caruso, A.; Voisin-Chiret, A.S.; Lancelot, J.C.; Sinicropi, M.S.; Garofalo, A.; Rault S. “Novel and Efficient Synthesis of 5,8-Dimethyl-9*H*-carbazol-3-ol via a Hydroxydeboronation Reaction.” **Heterocycles** 2007, 71(10), 2203–2210.
241. Aebly, A.H.; Levy, J.N.; Steger, B.J.; Quirke, J.C.; Belitsky, J.M. “Expedient Synthesis of Eumelanin-Inspired 5,6-Dihydroxyindole-2-Carboxylate Ethyl Ester Derivatives.” **RSC Adv.** 2018, 8(50), 28323–28328.
242. Pigza, J.A.; Han, J.S.; Chandra, A.; Mutnick, D.; Pink, M.; Johnston, J.N. “Total Synthesis of the Lycopodium Alkaloid Serratezomine A Using Free Radical-Mediated Vinyl Amination to Prepare a  $\beta$ -Stannyl Enamine Linchpin.” **J. Org. Chem.** 2013, 78(3), 822–843.
243. Luo, Z.; Jiang, Z.; Jiang, W.; Lin D. “C–H Amination of Purine Derivatives via Radical Oxidative Coupling.” **J. Org. Chem.** 2018, 83(7), 3710–3718.

244. Zhang, Q.; Chang, G.; Zhang, L. "Synthesis and Properties of Novel Heat-Resistant Fluorescent Conjugated Polymers with Bisindolylmaleimide." **Chinese Chem. Lett.** 2018, 29(3), 513–516.
245. Esposito, F.; Sechi, M.; Pala, N.; Sanna, A.; Koneru, P.C.; Kvaratskhelia, M.; et al. "Discovery of Dihydroxyindole-2-Carboxylic Acid Derivatives as Dual Allosteric HIV-1 Integrase and Reverse Transcriptase Associated Ribonuclease H Inhibitors." **Antivir. Res.** 2020, 174, 104671.
246. Krüger, A.; Gonçalves Maltarollo, V.; Wrenger, C.; Kronenberger, T. "ADME Profiling in Drug Discovery and a New Path Paved on Silica." *In Drug Discovery and Development—New Advances*; Gaitonde, V., Karmakar, R., Trivedi, A., Eds.; IntechOpen: London, UK, 2019; Volume 1, pp. 1–32.
247. Yang, H.; Lou, C.; Sun, L.; Li, J.; Cai, Y.; Wang, Z.; et al. "admetSAR 2.0: Web-Service for Prediction and Optimization of Chemical ADMET Properties." **Bioinformatics** 2018, 35, 1067–1069.
248. Cheng, F.; Li, W.; Zhou, Y.; Shen, J.; Wu, Z.; Liu, G.; Lee, P.W.; Tang, Y. "AdmetSAR: A Comprehensive Source and Free Tool for Assessment of Chemical ADMET Properties." **J. Chem. Inf. Model.** 2012, 52, 3099–3105.
249. Pires, D.E.V.; Blundell, T.L.; Ascher, D.B. "pkCSM: Predicting Small-Molecule Pharmacokinetic and Toxicity Properties Using Graph-Based Signatures." **J. Med. Chem.** 2015, 58, 4066–4072.
250. Shirato, K.; Kawase, M.; Matsuyama, S. "Wild-type Human Coronaviruses Prefer Cell-surface TMPRSS2 to Endosomal Cathepsins for Cell Entry." **J. Virol.** 2020, 517, 9–15.
251. Eleftheriou, P.; Amanatidou, D.; Petrou, A.; Geronikaki, A. "In Silico Evaluation of the Effectivity of Approved Protease Inhibitors against the Main Protease of the Novel SARS-CoV-2 Virus." **Molecules** 2020, 25, 2529.
252. Dong, M.; Zhang, J.; Ma, X. "ACE2, TMPRSS2 Distribution and Extrapulmonary Organ Injury in Patients with COVID-19." **Biomed. Pharmacother.** 2020, 131, 110678.
253. Giuzio, F.; Bonomo, M.G.; Catalano, A.; Infantino, V.; Salzano, G.; Monné, M.; et al. "Potential PDE4B inhibitors as promising candidates against SARS-CoV-2 infection". **Biomol. Concepts** 2023, 14(1), 20220033.